



# Palladium $\beta$ -diiminate chemistry: Reactivity towards monodentate ligands and arylboronic acids

Vincent T. Annibale, Runyu Tan, John Janetzko, Liisa M. Lund, Datong Song\*

Davenport Chemical Research Laboratories, Department of Chemistry, University of Toronto, 80 St. George Street, Toronto, Ontario, Canada M5S 3H6

## ARTICLE INFO

### Article history:

Available online 2 October 2011

Young Investigator Award Special Issue

### Keywords:

$\beta$ -Diiminate ligands  
Palladium  
Reactivity  
Monodentate ligands  
Boronic acids  
Nacnac

## ABSTRACT

Here we report the synthesis and characterization of a series of palladium  $\beta$ -diiminate complexes. Chloro-bridged dimers  $[\text{Pd}(\text{Ar}_2\text{nacnac})(\mu\text{-Cl})_2]$  (where  $[\text{Ar}_2\text{nacnac}]^-$  is  $[(\text{ArNC}(\text{CH}_3)_2\text{CH})^-]$  with Ar being aryl substituents) can serve as versatile starting materials, and can be cleaved by neutral monodentate ligands (L) to form mononuclear complexes  $[\text{Pd}(\text{Ar}_2\text{nacnac})(\text{L})\text{Cl}]$ , or engage in unusual transmetallation reactions with boronic acids to form tetrapallada-macrocycles. The reactivity of the tetrapallada-macrocyclic complexes towards L-type ligands, as well as the reactivity of  $[\text{Pd}(\text{Ar}_2\text{nacnac})(\text{L})\text{Cl}]$  complexes towards boronic acids was also explored.

© 2011 Elsevier B.V. All rights reserved.

## 1. Introduction

Aryl-substituted  $\beta$ -diiminate ligands (commonly referred to as “nacnac” ligands since they are bidentate, monoanionic N-donor ligands derived from acetylacetonate (acac)) are used extensively in inorganic and organometallic chemistry [1]. Nacnac complexes have been reported for elements across the periodic table, and interest continues since the nacnac ligands have been found to stabilize metals in unusual oxidation states and coordination environments, and find use in active catalytic systems [1]. Varying the “Ar” groups of the  $[\text{Ar}_2\text{nacnac}]^-$  ligands, see Fig. 1B, allows for the sterics and electronics of the ligand environment to be easily tuned.

Palladium nacnac chemistry prior to our initial work in the area was limited to a few well characterized examples. These earlier examples include the fully characterized complexes  $[\text{Pd}(\text{iPr}_2\text{nacnac})_2]$  [2],  $[\text{Pd}(\eta^3\text{-C}_3\text{H}_5)(\text{iPr}_2\text{nacnac})]$  [2], the unstable complex  $[\text{Pd}(\text{acac})(\text{Ar}_2\text{nacnac})]$  where (Ar) = 2,6-diisopropylphenyl that isomerizes into  $[\text{Pd}(\text{acac})(\kappa^2\text{-C,N-Ar}_2\text{nacnac})]$  [2],  $[\text{Pd}(\text{Ar}_2\text{nacnac})\text{ClMe}]$  [3], and the dinuclear complex  $[(\text{CH}_3\text{CN})_3\text{Pd}\{-\mu\text{-CH}(\text{C}(\text{Me})\text{NAr})_2\}\text{Pd}(\text{CH}_3\text{CN})_2]$  ( $\text{BF}_4$ )<sub>3</sub> [4]. Monomethylpalladium nacnac complexes where benzene C–H activation and migratory insertion of olefins are competitive have also been studied [5].

Our initial discovery in 2008 of a Pd nacnac chloro-bridged dimer, complex **1a** [6], has led to an expansion of the chemistry by allowing easy access to a host of mono-, and multi-nuclear Pd nacnac species [6,7]. Cleavage of **1a** with suitable monodentate ligands (L) allows easy access to mononuclear species of the general form  $[\text{Pd}(\text{Ph}_2\text{nacnac})(\text{Cl})(\text{L})]$  [6]. Reactions of **1a** with 4-tertbutylaniline can generate bimetallic and trimetallic complexes with chloro-amido double bridges over time [7].

In our recent investigations into palladium nacnac chemistry, we have explored the reactivity of  $[\text{Pd}(\text{Ph}_2\text{nacnac})(\text{Cl})(\text{L})]$  towards various transmetallation reagents, aiming to generate olefin polymerization pre-catalysts,  $[\text{Pd}(\text{Ph}_2\text{nacnac})(\text{R})(\text{L})]$ , where R is an alkyl or aryl group. Alternatively we have proposed that that if a suitable transmetallation reagent could replace the chloride ligands from **1a** itself, the resulting coordinatively unsaturated organopalladium species “[Pd(Ph<sub>2</sub>nacnac)(R)]” or its oligomers might be used directly as activator-free olefin polymerization catalysts. Our interest in the reactivity of **1a** towards transmetallation reagents led to the discovery of an unusual self-assembly when boronic acids were used. We reported the formation of a tetrapallada-macrocyclic induced by an unusual transmetallation, in which an anionic bidentate chelating nacnac ligand is replaced by a phenyl ligand from phenylboronic acid, leaving the chloride ligands intact [8]. The reactivity of these tetrapallada-macrocycles towards L-type ligands is presented in this paper. In addition, we detail the syntheses and characterization of a series of new Pd nacnac complexes where we expand upon the reactivity of Pd

\* Corresponding author. Tel.: +1 416 978 7014; fax: +1 416 978 7013.

E-mail address: [dsong@chem.utoronto.ca](mailto:dsong@chem.utoronto.ca) (D. Song).

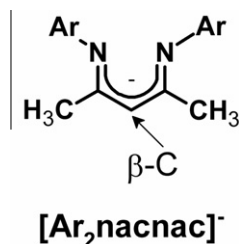


**Fig. 1.** Generic structure of [Ar<sub>2</sub>nacnac]<sup>-</sup> ligands where the β-C is noted. We refer to the central carbon of the [Ar<sub>2</sub>nacnac]<sup>-</sup> ligand as the β-C since it is β to the heteroatom in the free ligand, we extend this convention to metal complexes as well in order to avoid confusion.

nacnac complexes towards monodentate ligands and boronic acids.

## 2. Experimental

### 2.1. Materials and methods

All experimental procedures were performed in air unless otherwise stated. Air or moisture sensitive reactions were performed under dry nitrogen or argon with conventional glovebox or Schlenk techniques. [Pd(Ph<sub>2</sub>nacnac)(μ-Cl)]<sub>2</sub> (**1a**) [6], H[Ph<sub>2</sub>nacnac] [9], H[DippH<sub>2</sub>nacnac] (where DippH = diisopropylphenyl) [4,10], H[Ar<sup>F</sup><sub>2</sub>nacnac] (where Ar<sup>F</sup> = 3,5-bis(trifluoromethyl)phenyl) [11], Pd(PhCN)<sub>2</sub>Cl<sub>2</sub> [12], *trans*-[Pd(THT)<sub>2</sub>(C<sub>6</sub>F<sub>5</sub>)<sub>2</sub>] (where THT = tetrahydrothiophene) [13], [(Ph)Pd(μ-Cl)<sub>2</sub>Pd(Ph<sub>2</sub>nacnac)]<sub>2</sub> (**7a**) [8], pentafluorophenylboronic acid [14], [Pd(Ph<sub>2</sub>nacnac)(Py)Cl] (**4a**) [8] were prepared according to literature procedures. Other reagents were obtained from commercial sources and used as received. THF and benzene-*d*<sub>6</sub> was dried over Na/benzophenone and vacuum transferred before use. Dry and degassed pyridine and CH<sub>2</sub>Cl<sub>2</sub> for experiments where their use is specified was dried over CaH<sub>2</sub> and vacuum transferred before use. Toluene was dried after passing through a Pure Solv Innovative Technology Grubbs'-type solvent purification system, and degassed through three consecutive freeze-pump-thaw cycles. <sup>1</sup>H, <sup>11</sup>B, <sup>13</sup>C, <sup>19</sup>F NMR spectra were recorded on a Varian 400 MHz, or 300 MHz NMR instrument. All chemical shifts are reported in parts per million (δ) and the residual protio-solvent peaks were used as a reference (<sup>1</sup>H NMR, δ, ppm: dichloromethane-*d*<sub>2</sub>, 5.32; chloroform-*d*, 7.26; benzene-*d*<sub>6</sub>, 7.16; acetone-*d*<sub>6</sub>, 2.05. <sup>13</sup>C NMR, δ, ppm: dichloromethane-*d*<sub>2</sub>, 53.8; chloroform-*d*, 77.16; benzene-*d*<sub>6</sub>, 175.82; acetone-*d*<sub>6</sub>, 29.84, 206.26). <sup>11</sup>B NMR spectra were referenced using an external standard of KBF<sub>4</sub> in D<sub>2</sub>O (0.29 M) flame sealed in a glass capillary (<sup>11</sup>B NMR, δ, ppm: 0.00). Elemental analysis was performed by ANALEST at the University of Toronto.

### 2.2. X-ray crystallography

The X-ray diffraction data for structures **1b**, **1c**·(CH<sub>2</sub>Cl<sub>2</sub>), **2**, **4b**, **5**·(CH<sub>2</sub>Cl<sub>2</sub>), **6** were collected [15] on a Nonius Kappa-CCD diffractometer and processed with the DENZOSMN package [16]. The X-ray diffraction data for structures **3**, **4c**·0.5(CH<sub>2</sub>Cl<sub>2</sub>), **7b**, *trans*-[Pd(Py)<sub>2</sub>(Ph)Cl], **8**, **9** were collected on a Bruker Kappa Apex II diffractometer, and processed with the Bruker Apex 2 software package [17]. All data were collected with graphite monochromated Mo Kα radiation (λ = 0.71073 Å), at 150 K controlled by an Oxford Cryostream 700 series low temperature system. All structures were solved by the direct methods or Patterson method and refined using SHELXTL V6.10 [18]. Disordered CF<sub>3</sub> groups and CH<sub>2</sub>Cl<sub>2</sub> solvent molecules were modelled successfully. The crystallographic data are summarized in Table 1.

### 2.3. Preparation of complexes

#### 2.3.1. Synthesis of [Pd(DippH<sub>2</sub>nacnac)(μ-Cl)]<sub>2</sub> (**1b**)

H[DippH<sub>2</sub>nacnac] (48 mg, 0.11 mmol) and Pd(PhCN)<sub>2</sub>Cl<sub>2</sub> (38 mg, 0.099 mmol) were dissolved in 5 mL of methanol, KOtBu (11 mg, 0.099 mmol) was then added. The mixture was stirred overnight and the precipitate changed colour from red to brown and finally to green. The precipitated product was filtered off and washed with a small amount of methanol. [Pd(DippH<sub>2</sub>nacnac)Cl]<sub>2</sub> (**1b**) was obtained in 58% yield (38 mg). The crystals suitable for X-ray crystallographic analysis were obtained by layering a CH<sub>2</sub>Cl<sub>2</sub> solution (approximately 8 mg of **1b** in 0.1 mL of CH<sub>2</sub>Cl<sub>2</sub>) with methanol (~3.5 mL) at -30 °C.

<sup>1</sup>H NMR (400 MHz, CD<sub>2</sub>Cl<sub>2</sub>): δ 7.01 (m, 4H), 6.83 (m, 8H), 4.68 (s, 2H, nacnac β-CH), 3.09 (septet, 8H, -CHMe<sub>2</sub>), 1.44 (s, 12H, nacnac-CH<sub>3</sub>), 1.29 (d, 24H, J = 6.9 Hz, -CH(CH<sub>3</sub>)<sub>2</sub>), 1.05 (d, 24H, J = 6.9 Hz, -CH(CH<sub>3</sub>)<sub>2</sub>). <sup>13</sup>C NMR (75 MHz, CD<sub>2</sub>Cl<sub>2</sub>): δ 155.93, 145.93, 142.59, 126.69, 123.92, 94.17, 28.48, 24.46, 24.06, 23.53. *Anal. Calc.* for (C<sub>58</sub>H<sub>82</sub>Cl<sub>2</sub>N<sub>4</sub>Pd<sub>2</sub>)·(CH<sub>3</sub>OH): C, 61.56; H, 7.53; N, 4.87. *Found:* C, 61.46; H, 7.06; N, 4.88%.

#### 2.3.2. Synthesis of [Pd(Ar<sup>F</sup><sub>2</sub>nacnac)(μ-Cl)]<sub>2</sub> (**1c**) and [Pd(Ar<sup>F</sup><sub>2</sub>nacnac)]<sub>2</sub> (**2**)

A milky white suspension of H[Ar<sup>F</sup><sub>2</sub>nacnac] (1.412 g, 2.7 mmol) and KOtBu (281 mg, 2.58 mmol) in methanol (9 mL) was added dropwise to a stirred solution of Na<sub>2</sub>PdCl<sub>4</sub> (788 mg, 2.67 mmol) in methanol (4 mL). The mixture was stirred overnight resulting in a dark brown precipitate which was collected by filtration and washed with water, followed by methanol. The crude brown precipitate is a 2:5 mixture of [Pd(Ar<sup>F</sup><sub>2</sub>nacnac)]<sub>2</sub> (**2**) to [Pd(Ar<sup>F</sup><sub>2</sub>nacnac)(μ-Cl)]<sub>2</sub> (**1c**) by <sup>1</sup>H, and <sup>19</sup>F NMR spectroscopy. The crude brown solid (~1.3 g) was dissolved in a minimal amount of diethyl ether (~4 mL) in a vial, and hexanes (~15 mL) was layered on top, after ~1 h the majority of the red crystals of **2** began to form at the bottom of vial resulting in a greenish brown supernatant which was transferred off and chilled to -30 °C. After 20 min at -30 °C a second crop of red crystals had formed leaving an emerald green supernatant containing primarily **1c**. The red crystals from the two crops were redissolved in a minimal amount of CHCl<sub>3</sub> (~1 mL) and layered with hexanes (~10 mL) and chilled to -30 °C, this resulted in crystals suitable for X-ray crystallographic analysis, and elemental analysis after drying under vacuum. The yield of recrystallized **2** was 6% (172 mg). The solvent was removed from the emerald green supernatant, the residue was re-crystallized from a minimal amount of CHCl<sub>3</sub> (~2 mL), layered with hexanes (~15 mL), and chilled to -30 °C. Green crystals suitable for X-ray crystallographic analysis were obtained from slow evaporation of a CH<sub>2</sub>Cl<sub>2</sub> solution of **1c**. The yield of recrystallized **1c** was 25% (867 mg).

Characterization of Pd(Ar<sup>F</sup><sub>2</sub>nacnac)(μ-Cl)]<sub>2</sub> (**1c**): <sup>1</sup>H NMR (400 MHz, acetone-*d*<sub>6</sub>): δ 7.65 (s, 4H), 7.56 (d, 8H, J = 1.4 Hz), 5.00 (s, 2H, nacnac β-CH), 1.62 (s, 12H, nacnac-CH<sub>3</sub>). <sup>19</sup>F NMR (376 MHz, acetone-*d*<sub>6</sub>): δ -64.26 (s, 24F, -CF<sub>3</sub>). <sup>13</sup>C NMR (100 MHz, acetone-*d*<sub>6</sub>): δ 158.38, 152.19, 131.91, 125.36, 122.66, 119.96, 99.82, 23.8. *Anal. Calc.* for C<sub>42</sub>H<sub>26</sub>N<sub>2</sub>F<sub>24</sub>Cl<sub>2</sub>Pd<sub>2</sub>: C, 38.03; H, 1.98; N, 4.22. *Found:* C, 38.18; H, 1.95; N, 4.30%.

Characterization of [Pd(Ar<sup>F</sup><sub>2</sub>nacnac)]<sub>2</sub> (**2**): <sup>1</sup>H NMR (300 MHz, acetone-*d*<sub>6</sub>): δ 7.74 (d, 8H, J = 1.3 Hz), 7.64 (s, 4H), 5.61 (s, 2H, nacnac β-CH), 1.86 (s, 12H, nacnac-CH<sub>3</sub>). <sup>19</sup>F NMR (376 MHz, acetone-*d*<sub>6</sub>): δ -64.55 (s, 24F, -CF<sub>3</sub>). <sup>13</sup>C NMR (75 MHz, acetone-*d*<sub>6</sub>): δ 163.60, 150.93, 132.04, 131.60, 125.82, 112.89, 22.58. *Anal. Calc.* for C<sub>42</sub>H<sub>26</sub>N<sub>2</sub>F<sub>24</sub>Pd<sub>2</sub>: C, 43.90; H, 2.28; N, 4.88. *Found:* C, 43.63; H, 2.29; N, 4.94%.

#### 2.3.3. Synthesis of [Pd((PhN=C(CH<sub>3</sub>))<sub>2</sub>CH<sub>2</sub>)(C<sub>6</sub>F<sub>5</sub>)<sub>2</sub>] (**3**)

In a Schlenk flask under argon *trans*-Pd(THT)<sub>2</sub>(C<sub>6</sub>F<sub>5</sub>)<sub>2</sub> (303 mg, 0.49 mmol) and [Ph<sub>2</sub>nacnac]H (127 mg, 0.50 mmol) were dissolved

**Table 1**  
Crystallographic data.

|   | <b>1b</b>   | <b>1c</b> · (CH <sub>2</sub> Cl <sub>2</sub> )   | <b>2</b>   | <b>3</b>  |
|---|---|--|--|---|
| Formula                                 | C <sub>58</sub> H <sub>82</sub> Cl <sub>2</sub> N <sub>4</sub> Pd <sub>2</sub>                | C <sub>44</sub> H <sub>26</sub> Cl <sub>6</sub> F <sub>24</sub> N <sub>4</sub> Pd <sub>2</sub> | C <sub>42</sub> H <sub>26</sub> F <sub>24</sub> N <sub>4</sub> Pd                | C <sub>29</sub> H <sub>18</sub> F <sub>10</sub> N <sub>2</sub> Pd                                 |
| Formula weight                          | 1118.98   | 1492.19  | 1149.07  | 690.85  |
| T (K)                                   | 150(2)  | 150(2)   | 150(2)   | 150(2)  |
| Space group                             | P2 <sub>1</sub> /n  | P2 <sub>1</sub> /n   | P2 <sub>1</sub> /n   | P2 <sub>1</sub> /n  |
| a (Å)                                   | 9.1465(18)  | 11.428(2)  | 14.571(3)  | 9.2861(2)   |
| b (Å)                                   | 14.233(3)   | 15.760(3)  | 8.6434(17)   | 20.7555(4)  |
| c (Å)                                   | 21.023(4)   | 15.404(3)  | 17.805(4)  | 14.2909(3)  |
| α (°)                                   | 90  | 90   | 90   | 90  |
| β (°)                                   | 92.36(3)  | 103.99(3)  | 108.52(3)  | 96.7330(10)   |
| γ (°)                                   | 90  | 90   | 90   | 90°   |
| V (Å <sup>3</sup> )                     | 2734.5(9)   | 2692.3(9)  | 2126.3(7)  | 2735.40(10)   |
| Z                                       | 2   | 2  | 2  | 4   |
| D <sub>calc</sub> (g cm <sup>-3</sup> ) | 1.359   | 1.841  | 1.795  | 1.678   |
| μ (mm <sup>-1</sup> )                   | 0.795   | 1.086  | 0.581  | 0.769   |
| Number of reflections collected         | 19863   | 10366  | 13916  | 20988   |
| Number of independent reflections       | 6203  | 4454   | 3733   | 4791  |
| Goodness-of-fit (GOF) on F <sup>2</sup> | 1.005   | 1.276  | 1.013  | 1.034   |
| R [I > 2σ (I)]                          | R <sub>1</sub> = 0.0395<br>wR <sub>2</sub> = 0.0987   | R <sub>1</sub> = 0.0556<br>wR <sub>2</sub> = 0.1614  | R <sub>1</sub> = 0.0607<br>wR <sub>2</sub> = 0.1370                              | R <sub>1</sub> = 0.0213<br>wR <sub>2</sub> = 0.0526   |
| R (all data)                            | R <sub>1</sub> = 0.0628<br>wR <sub>2</sub> = 0.1143   | R <sub>1</sub> = 0.0679<br>wR <sub>2</sub> = 0.1705  | R <sub>1</sub> = 0.1162<br>wR <sub>2</sub> = 0.1656                              | R <sub>1</sub> = 0.0244<br>wR <sub>2</sub> = 0.0545   |
|   | <b>4b</b>   | <b>2(4c)</b> · (CH <sub>2</sub> Cl <sub>2</sub> )  | <b>5</b> · (CH <sub>2</sub> Cl <sub>2</sub> )                                    | <b>6</b>  |
| Formula                                 | C <sub>34</sub> H <sub>46</sub> ClN <sub>3</sub> Pd   | C <sub>53</sub> H <sub>36</sub> Cl <sub>4</sub> F <sub>24</sub> N <sub>6</sub> Pd <sub>2</sub> | C <sub>34</sub> H <sub>50</sub> Cl <sub>3</sub> N <sub>4</sub> O <sub>2</sub> Pd | C <sub>49</sub> H <sub>45</sub> BF <sub>4</sub> N <sub>6</sub> Pd                                 |
| Formula weight                          | 638.59  | 1567.48  | 759.53   | 911.12  |
| T (K)                                   | 150(2)  | 150(2)   | 150(2)   | 150(2)  |
| Space group                             | P1̄   | P2 <sub>1</sub> /n   | P1̄  | P2 <sub>1</sub> /c  |
| a (Å)                                   | 8.7150(17)  | 14.9527(4)   | 12.746(3)  | 9.6654(19)  |
| b (Å)                                   | 12.045(2)   | 16.7010(4)   | 12.972(3)  | 17.208(3)   |
| c (Å)                                   | 16.923(3)   | 24.4803(6)   | 13.036(3)  | 26.098(5)   |
| α (°)                                   | 75.78(3)  | 90   | 85.68(3)   | 90  |
| β (°)                                   | 83.29(3)  | 101.9270(10)   | 87.44(3)   | 96.32(3)  |
| γ (°)                                   | 68.89(3)  | 90   | 61.35(3)   | 90  |
| V (Å <sup>3</sup> )                     | 1605.7(6)   | 5981.4(3)  | 1886.1(6)  | 4314.3(15)  |
| Z                                       | 2   | 4  | 2  | 4   |
| D <sub>calc</sub> (g cm <sup>-3</sup> ) | 1.321   | 1.741  | 1.336  | 1.403   |
| μ (mm <sup>-1</sup> )                   | 0.687   | 0.897  | 0.738  | 0.490   |
| Number of reflections collected         | 12 163  | 46968  | 20933  | 38 581  |
| Number of independent reflections       | 5360  | 10 534   | 8527   | 9824  |
| Goodness-of-fit (GOF) on F <sup>2</sup> | 1.793   | 1.015  | 1.043  | 1.030   |
| R [I > 2σ (I)]                          | R <sub>1</sub> = 0.1262<br>wR <sub>2</sub> = 0.3007   | R <sub>1</sub> = 0.0444<br>wR <sub>2</sub> = 0.1035  | R <sub>1</sub> = 0.0372<br>wR <sub>2</sub> = 0.0862                              | R <sub>1</sub> = 0.0526<br>wR <sub>2</sub> = 0.1228   |
| R (all data)                            | R <sub>1</sub> = 0.1449<br>wR <sub>2</sub> = 0.3093   | R <sub>1</sub> = 0.0608<br>wR <sub>2</sub> = 0.1145  | R <sub>1</sub> = 0.0491<br>wR <sub>2</sub> = 0.0931                              | R <sub>1</sub> = 0.1089<br>wR <sub>2</sub> = 0.1516   |
|   | <b>7b</b>   | <i>Trans</i> -[Pd(Py) <sub>2</sub> (Ph)Cl]   | <b>8</b>   | <b>9</b>  |
| Formula                                 | C <sub>46</sub> H <sub>42</sub> Cl <sub>4</sub> F <sub>2</sub> N <sub>4</sub> Pd <sub>4</sub> | C <sub>16</sub> H <sub>15</sub> ClN <sub>2</sub> Pd  | C <sub>23</sub> H <sub>18</sub> ClF <sub>5</sub> N <sub>2</sub> Pd               | C <sub>114</sub> H <sub>102</sub> Cl <sub>8</sub> F <sub>10</sub> N <sub>12</sub> Pd <sub>8</sub> |
| Formula weight                          | 1256.24   | 377.15   | 559.24   | 2964.88   |
| T (K)                                   | 150(2)  | 150(2)   | 150(2)   | 150(2)  |
| Space group                             | C2/c  | C2/c   | P2 <sub>1</sub> 2 <sub>1</sub> 2 <sub>1</sub>                                    | P2 <sub>1</sub> /n  |
| a (Å)                                   | 21.3987(4)  | 22.9651(8)   | 12.1558(5)   | 12.7442(4)  |
| b (Å)                                   | 14.0182(3)  | 9.3409(3)  | 12.9993(5)   | 34.4264(10)   |
| c (Å)                                   | 18.7361(6)  | 16.0016(6)   | 13.5993(6)   | 13.9746(4)  |
| α (°)                                   | 90  | 90   | 90   | 90  |
| β (°)                                   | 124.7160(10)  | 118.9200(10)   | 90   | 115.3620(10)  |
| γ (°)                                   | 90  | 90   | 90   | 90  |
| V (Å <sup>3</sup> )                     | 4619.8(2)   | 3004.52(18)  | 2148.92(15)  | 5540.2(3)   |
| Z                                       | 4   | 8  | 4  | 2   |
| D <sub>calc</sub> (g cm <sup>-3</sup> ) | 1.806   | 1.668  | 1.729  | 1.777   |
| μ (mm <sup>-1</sup> )                   | 1.809   | 1.403  | 1.044  | 1.532   |
| Number of reflections collected         | 17 232  | 13 346   | 16 125   | 36 981  |
| Number of independent reflections       | 4067  | 3446   | 3784   | 9756  |
| Goodness-on fit (GOF) on F <sup>2</sup> | 1.028   | 0.958  | 1.019  | 1.003   |
| R [I > 2σ (I)]                          | R <sub>1</sub> = 0.0250<br>wR <sub>2</sub> = 0.0548   | R <sub>1</sub> = 0.0445<br>wR <sub>2</sub> = 0.0734  | R <sub>1</sub> = 0.0319<br>wR <sub>2</sub> = 0.0561                              | R <sub>1</sub> = 0.0420<br>wR <sub>2</sub> = 0.0932   |
| R (all data)                            | R <sub>1</sub> = 0.0375<br>wR <sub>2</sub> = 0.0597   | R <sub>1</sub> = 0.0917<br>wR <sub>2</sub> = 0.0852  | R <sub>1</sub> = 0.0417<br>wR <sub>2</sub> = 0.0589                              | R <sub>1</sub> = 0.0666<br>wR <sub>2</sub> = 0.1036   |

in 20 mL of dry and degassed toluene and heated to reflux overnight. After cooling the workup was performed in air, the reaction mixture was filtered through Celite and the filtrate was concentrated under vacuum. Hexanes (~100 mL) was added to the filtrate to cause a white microcrystalline precipitate to form, the

precipitate was collected by filtration and washed with hexanes, and dried under vacuum. The yield of **3** was 50% (175 mg). Crystals suitable for X-ray crystallographic analysis were grown by layering a concentrated CH<sub>2</sub>Cl<sub>2</sub> solution of **3** (approximately 8 mg of **3** in 0.1 mL of CH<sub>2</sub>Cl<sub>2</sub>) with methanol (~3.5 mL) at -30 °C. <sup>1</sup>H NMR

(400 MHz, acetone- $d_6$ ):  $\delta$  7.26–7.23 (m, 4H), 7.16–7.12 (m, 2H), 6.76–6.74 (m, 4H), 4.46 (s, 2H,  $\beta$ -CH $_2$ ), 2.30 (s, 6H,  $\beta$ -diimine CH $_3$ ).  $^{19}\text{F}$  NMR (376 MHz, acetone- $d_6$ ):  $\delta$  -116.54 (dd, 4F,  $J = 5.5$  Hz,  $J = 27.4$  Hz), -165.11 (t, 2F,  $J = 19.6$  Hz), -168.8 to -168.95 (m, 4F).  $^{13}\text{C}$  NMR (100 MHz, acetone- $d_6$ ):  $\delta$  177.54, 149.08, 129.43, 126.80, 122.21, 51.71, 24.75. *Anal. Calc.* for  $\text{C}_{29}\text{H}_{18}\text{F}_{10}\text{N}_2\text{Pd}$ : C, 50.42; H, 2.63; N, 4.05. Found: C, 50.33; H, 2.64; N, 4.21%.

### 2.3.4. Synthesis of [Pd(Diph $_2$ nacnac)(Py)Cl] (**4b**)

In air, pyridine (0.10 mL, 1.2 mmol) was added to a dark green solution of **1b** (50 mg, 0.045 mmol) in 10 mL of  $\text{CHCl}_3$ . The initially green solution was heated at 70 °C, gradually the colour changed to brown and finally to bright red after 3 h of heating. The solvent and volatiles were removed under vacuum and the residue was washed with hexanes, and the residue was recrystallized from a  $\text{CH}_2\text{Cl}_2$ /pentane solvent mixture. The orange-red crystals of [Pd(Diph $_2$ nacnac)(Py)Cl] (**4b**) were dried under vacuum; the yield was 70% (40 mg). Crystals suitable for X-ray crystallographic analysis were grown by slow evaporation of a  $\text{CH}_2\text{Cl}_2$  solution of **4b**.  $^1\text{H}$  NMR (400 MHz,  $\text{CDCl}_3$ ):  $\delta$  7.89 (dd, 2H,  $J = 1.5$  Hz,  $J = 6.5$  Hz), 7.36 (tt, 1H,  $J = 1.4$  Hz,  $J = 7.7$  Hz), 7.14 (dd, 1H,  $J = 6.7$  Hz,  $J = 8.4$  Hz), 7.07–7.00 (m, 3H), 6.88 (d, 2H,  $J = 7.7$  Hz), 6.85 (dd, 2H,  $J = 6.6$  Hz,  $J = 7.5$  Hz), 4.90 (s, 1H, nacnac  $\beta$ -CH), 3.61 (septet, 2H, -CHMe $_2$ ), 3.42 (septet, 2H, -CHMe $_2$ ), 1.70 (s, 3H, nacnac-CH $_3$ ), 1.66 (s, 3H, nacnac-CH $_3$ ), 1.51 (d, 6H,  $J = 6.8$  Hz, -CH(CH $_3$ ) $_2$ ), 1.22 (d, 6H,  $J = 6.9$  Hz, -CH(CH $_3$ ) $_2$ ), 1.16 (dd, 12H,  $J = 1.5$  Hz,  $J = 6.8$  Hz, -CH(CH $_3$ ) $_2$ ).  $^{13}\text{C}$  NMR (100 MHz,  $\text{CDCl}_3$ ):  $\delta$  158.32, 157.40, 152.27, 148.81, 146.42, 143.49, 142.58, 136.47, 126.38, 125.73, 123.74, 123.65, 122.87, 95.50, 28.48, 28.05, 24.81, 24.60, 24.39, 24.20.

*Anal. Calc.* for  $(\text{C}_{34}\text{H}_{46}\text{ClN}_3\text{Pd}) \cdot 0.5(\text{CH}_2\text{Cl}_2)$ : C, 60.84; H, 6.96; N, 6.17. Found: C, 60.40; H, 6.41; N, 6.16.

### 2.3.5. Synthesis of [Pd(Ar $^F$ nacnac)(Py)Cl] (**4c**)

In air, pyridine (73  $\mu\text{L}$ , 0.90 mmol) was added to a dark green solution of **1c** (187 mg, 0.14 mmol) in 30 mL of  $\text{CH}_2\text{Cl}_2$ , which turned orange within a minute. The reaction mixture was stirred for 15 min and the solvent and volatiles were removed under vacuum. The residue was washed with hexanes, and the material was recrystallized from a  $\text{CH}_2\text{Cl}_2$ /pentane solvent mixture. The orange-red crystals of **4c** were dried under vacuum; the yield was 88% (185 mg). Crystals suitable for X-ray crystallographic analysis were grown by slow evaporation of a  $\text{CH}_2\text{Cl}_2$  solution of **4c**.  $^1\text{H}$  NMR (400 MHz,  $\text{CDCl}_3$ ):  $\delta$  8.60 (m, 1H), 8.24 (m, 2H), 7.63 (m, 2H), 7.51 (m, 2H), 7.43 (m, 2H), 7.30 (m, 2H), 6.92 (m, 2H), 4.86 (s, 1H, nacnac  $\beta$ -CH), 1.73 (s, 3H, nacnac-CH $_3$ ), 1.72 (s, 3H, nacnac-CH $_3$ ).  $^{19}\text{F}$  NMR (376 MHz,  $\text{CDCl}_3$ ):  $\delta$  -63.03 (s, 6F), -63.49 (s, 6F).  $^{13}\text{C}$  NMR (100 MHz,  $\text{CDCl}_3$ ):  $\delta$  159.53, 157.34, 152.67, 152.17, 151.93, 149.83, 137.58, 135.87, 131.89, 131.56, 131.02, 130.69, 127.89, 126.89, 124.95, 118.71, 118.18, 98.43, 24.83, 23.78. *Anal. Calc.* for  $\text{C}_{26}\text{H}_{18}\text{N}_3\text{F}_{12}\text{ClPd}$ : C, 42.07; H, 2.44; N, 5.66. Found: C, 42.08; H, 2.58; N, 5.91%.

### 2.3.6. Synthesis of O $_2$ -activation product [Pd(L1)Cl(Me-Im)] (**5**), (poor reproducibility)

In air, **1b** (22 mg, 0.02 mmol) and 1-methylimidazole (Me-Im, 3.25  $\mu\text{L}$ , 0.04 mmol) were dissolved in 10 mL of  $\text{CH}_2\text{Cl}_2$ , after 2 months at R.T. red X-ray diffraction quality crystals of [Pd(L1)Cl(Me-Im)] (**6**) were obtained and the  $^1\text{H}$  NMR spectrum was recorded.  $^1\text{H}$  NMR (400 MHz,  $\text{CD}_2\text{Cl}_2$ ):  $\delta$  7.93 (s, 1H), 7.29–7.06 (m, 6H), 6.82 (m, 1H), 5.02 (s, 1H), 3.66 (s, 3H), 3.60 (septet, 1H,  $J = 13.7$ , 6.8 Hz), 3.48 (septet, 1H,  $J = 13.7$ , 6.8 Hz), 3.25 (septet, 1H,  $J = 13.7$ , 6.8 Hz), 2.79 (septet, 1H,  $J = 13.7$ , 6.8 Hz), 2.04 (s, 3H), 1.81 (s, 2H), 1.51 (d, 3H,  $J = 6.7$  Hz), 1.29 (d, 3H,  $J = 6.8$  Hz), 1.25 (d, 3H,  $J = 6.9$  Hz), 1.21 (d, 3H,  $J = 6.7$  Hz), 1.11 (d, 3H, 6.9 Hz), 1.04 (dd, 6H,  $J = 6.7$ , 4.7 Hz).

### 2.3.7. Synthesis of [Pd(Ph $_2$ nacnac)(L $_2$ ) $_2$ ]BF $_4$ (**6**)

[Pd(Ph $_2$ nacnac)( $\mu$ -Cl)] $_2$  (**1a**) (29.9 mg, 0.0382 mmol) and *N*-methyl-4,5-diphenylimidazole (**L2**; 34.9 mg, 0.149 mmol) were added to a Schlenk flask, which was then purged with argon. Dry THF (10 mL) was added, and the solution turned from dark green to orange within a minute. Sodium tetrafluoroborate (8.6 mg, 0.0783 mmol) was added to the reaction mixture after 30 min, and the solution was stirred overnight. The solution was gravity filtered, and the solvent was removed from the filtrate under vacuum to leave an orange residue. The residue was further washed with water and hexanes and dried under vacuum to give an orange powder. Yield 81% (56.4 mg). Crystals suitable for X-ray crystallographic analysis were grown by slow vapour diffusion of hexanes into a concentrated THF solution of [Pd(Ph $_2$ nacnac)(L $_2$ ) $_2$ ]BF $_4$  (**6**) (~10 mg of **6** in 0.1 mL of THF).  $^1\text{H}$  NMR (400 MHz,  $\text{CD}_2\text{Cl}_2$ ):  $\delta$  7.69–6.89 (m, 30H, aromatic C–H), 5.39 (s, 2H, imidazole C–H), 5.09 (s, 1H, nacnac  $\beta$ -H), 2.85 (s, 6H, imidazole CH $_3$ ), 1.87 (s, 6H, nacnac CH $_3$ ).  $^{13}\text{C}$  NMR (100 MHz,  $\text{CD}_2\text{Cl}_2$ ):  $\delta$  24.3, 30.6, 33.5, 98.4, 125.6, 125.9, 127.3, 127.8, 128.6, 128.7, 128.8, 128.9, 129.5, 129.7, 130.7, 132.7, 136.2, 139.4, 151.2, 159.2. *Anal. Calc.* for  $\text{C}_{49}\text{H}_{45}\text{BF}_4\text{N}_6\text{Pd}$ : C, 64.60; H, 4.98; N, 9.23. Found: C, 64.43; H, 5.44; N, 8.77%.

### 2.3.8. Synthesis of [(4-FPh)Pd( $\mu$ -Cl) $_2$ Pd(Ph $_2$ nacnac)] $_2$ (**7b**)

Following a procedure similar to that described previously for the synthesis of **7a** [8], in air and with non-anhydrous solvents and reagents directly from commercial sources, **1a** (50 mg, 0.064 mmol) was dissolved in 1 mL of a benzene:acetone solvent mixture (9:1 v/v) and transferred to a 4 mL vial containing 4-fluorophenylboronic acid (11.5 mg, 0.082 mmol). After mixing the vial was sealed and gradually heated to 75 °C. After heating overnight, rhombus-shaped, orange, X-ray quality single crystals of [(4-FPh)Pd( $\mu$ -Cl) $_2$ Pd(Ph $_2$ nacnac)] $_2$  (**7b**) deposited on the insides of the vial. The mother-liquor was aspirated off and the crystals of **7b** were washed with benzene, followed by hexanes and dried in vacuum. The yield was 47% (19.7 mg). Because of poor solubility not all  $^{13}\text{C}$  resonances are visible even after overnight scans.

$^1\text{H}$  NMR (400 MHz,  $\text{CD}_2\text{Cl}_2$ ):  $\delta$  7.88–7.96 (m, 2 H), 7.45–7.52 (m, 4 H), 7.30–7.41 (m, 10 H), 7.19–7.28 (m, 4 H), 7.05–7.11 (m, 4 H), 6.90–6.98 (m, 2 H), 6.73–6.82 (m, 2 H), 3.89 (s, 2 H), 2.07 (s, 6H), 0.95 ppm (s, 6H).  $^{19}\text{F}$  NMR (376 MHz,  $\text{CD}_2\text{Cl}_2$ ):  $\delta$  -122.25 to -122.36 (m, 2F).

$^{13}\text{C}$  NMR (100 MHz,  $\text{CD}_2\text{Cl}_2$ ):  $\delta$  186.19, 129.36, 128.76, 127.15, 125.84, 124.76, 23.92, 23.35.

*Anal. Calc.* for  $\text{C}_{46}\text{H}_{42}\text{Cl}_4\text{F}_2\text{N}_4\text{Pd}_4$ : C, 43.98; H, 3.37; N, 4.46. Found: C, 44.58; H, 3.32; N, 4.51.

### 2.3.9. Synthesis of [Pd((PhN=C(CH $_3$ )) $_2$ CH $_2$ )Cl(C $_6$ F $_5$ )] (**8**) and trace octanuclear complex **9**

In a nitrogen-filled glovebox **1a** (64 mg, 0.082 mmol) and (C $_6$ F $_5$ )B(OH) $_2$  (22.1 mg, 0.10 mmol) were dissolved in 1.3 mL of dry, degassed, toluene. The reaction mixture was placed in a 7 mL vial, sealed, and heated in a 75 °C oil bath overnight. The yellow X-ray diffraction quality crystals of [Pd((PhN=C(CH $_3$ )) $_2$ CH $_2$ )Cl(C $_6$ F $_5$ )] (**8**) were collected by filtration, washed with toluene, pentane, and dried in vacuum. The yield was 54% (49 mg). The X-ray crystal structure of octanuclear Pd complex (**9**) was obtained from a trace amount of red–orange crystals also produced in this reaction. Poor solubility prevented  $^{13}\text{C}$  NMR data from being obtained for **8**.  $^1\text{H}$  NMR (400 MHz,  $\text{CDCl}_3$ ):  $\delta$  7.50–7.46 (m, 2H), 7.33–7.31(m, 1H), 7.23–7.21(m, 2H), 7.18–7.16 (m, 1H), 7.13–7.11 (m, 2H), 6.70–6.68 (m, 2H), 4.60 (s, 2H,  $\beta$ -CH $_2$ ), 2.24 (s, 3H,  $\beta$ -diimine CH $_3$ ), 2.23(s, 3H,  $\beta$ -diimine CH $_3$ ).  $^{19}\text{F}$  NMR (376 MHz,  $\text{CDCl}_3$ ):  $\delta$  -120.99 (m, 2F), -161.34 (t, 1F,  $J = 19.9$  Hz), -163.97 (m, 2F). *Anal. Calc.* for  $\text{C}_{23}\text{H}_{18}\text{ClF}_5\text{N}_2\text{Pd}$ : C, 49.39; H, 3.24; N, 5.01. Found: C, 49.16; H, 3.58; N, 4.83%.

#### 2.4. Cleavage of **7a** with pyridine yielding **4a**, and *trans*-[Pd(Py)<sub>2</sub>(Ph)Cl]

Performed in a nitrogen-filled glovebox with CH<sub>2</sub>Cl<sub>2</sub> and pyridine that had been dried over calcium hydride and vacuum-transferred prior to use. In a Pyrex bomb with a Teflon valve, **7a** (10 mg, 0.0082 mmol) was suspended in 5 mL of CH<sub>2</sub>Cl<sub>2</sub> and the mixture was sonicated for 1 h in order to dissolve the orange starting material. The bomb was brought back into the glovebox and pyridine (4 μL, 0.049 mmol) was added, after 10 min the solvent and volatiles were removed under vacuum, and NMR spectroscopy was performed. <sup>1</sup>H NMR spectroscopy of the mixture indicates that only **4a** and *trans*-[Pd(Py)<sub>2</sub>(Ph)Cl] form when compared with <sup>1</sup>H NMR spectral data reported for **4a** [8], and *trans*-[Pd(Py)<sub>2</sub>(Ph)Cl] [19]. Recrystallization of the mixture (~10 mg) from a CH<sub>2</sub>Cl<sub>2</sub> solution (~0.1 mL) layered with hexanes (~5 mL) at -30 °C gave X-ray diffraction quality crystals of both orange **4a**, and colourless *trans*-[Pd(Py)<sub>2</sub>(Ph)Cl].

#### 2.5. Reaction of **4a** with 1.2 equiv. phenylboronic acid

In a nitrogen-filled glovebox, in a J. Young NMR tube 19.0 mg (0.0403 mmol) of orange-red **4a** and 6.0 mg (0.0492 mmol) of phenylboronic acid were dissolved in 0.5 mL of dry and degassed C<sub>6</sub>D<sub>6</sub> and left at R.T. overnight giving a brown solution. <sup>1</sup>H NMR was performed, then a flame-sealed capillary containing a 0.29 M solution of KBF<sub>4</sub> in D<sub>2</sub>O was inserted and <sup>11</sup>B NMR was performed. See Supporting Information for NMR spectra.

<sup>1</sup>H NMR of **4a** (400 MHz, C<sub>6</sub>D<sub>6</sub>): δ 7.89–7.86 (m, 2H), 7.44–7.40 (m, 2H), 7.27–7.21 (m, 2H), 7.06–7.01 (m, 1H), 6.54–6.30 (m, 5H), 6.36–6.31 (m, 1H), 5.93–5.89 (m, 2H), 4.90 (s, 1H, nacnac β-CH), 1.77 (s, 3H, nacnac-CH<sub>3</sub>), 1.67 (s, 3H, nacnac-CH<sub>3</sub>).

<sup>1</sup>H NMR of **1a** (400 MHz, C<sub>6</sub>D<sub>6</sub>): δ 6.99–6.94 (m, 8H), 6.87–6.82 (m, 4H), 6.79–6.76 (m, 8H), 4.57 (s, 2H, nacnac β-CH), 1.45 (s, 12H, nacnac-CH<sub>3</sub>).

#### 2.6. Control experiments to determine stoichiometry of Lewis acid–base adduct from reaction of **4a** with phenylboronic acid

In a nitrogen-filled glovebox in a J. Young tube, solutions of phenylboronic acid in dry/degassed C<sub>6</sub>D<sub>6</sub> (final concentration

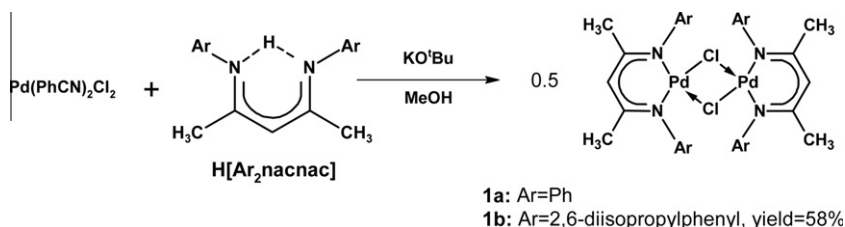
0.098 M), and solutions of pyridine in C<sub>6</sub>D<sub>6</sub> where combined such that the final volume of solution is 500 μL. The solutions were allowed to equilibrate for at least 1 h at R. T. before being subjected to <sup>1</sup>H NMR spectroscopy. Afterwards a flame-sealed capillary containing a 0.29 M solution of KBF<sub>4</sub> in D<sub>2</sub>O was inserted and <sup>11</sup>B NMR spectroscopy was performed. See Supporting Information for NMR spectra.

### 3. Results and discussion

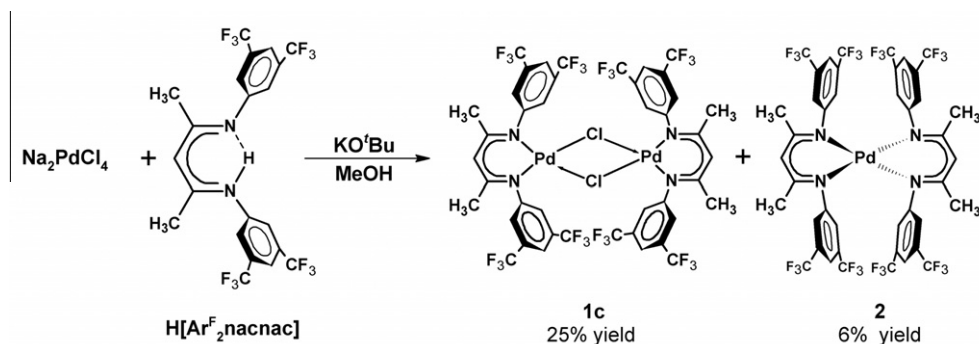
#### 3.1. Synthesis and characterization of [Pd(Ar<sub>2</sub>nacnac)(μ-Cl)]<sub>2</sub> complexes

An entry point into palladium nacnac chemistry is the synthesis of chloro-bridged dimers of the general form [Pd(Ar<sub>2</sub>nacnac)(μ-Cl)]<sub>2</sub>, these versatile starting materials allow simple access to other palladium nacnac complexes. Varying the Ar-groups of the [Ar<sub>2</sub>nacnac]<sup>-</sup> ligand allows for a comparison of the reactivities of these compounds. The reaction of H[Ar<sub>2</sub>nacnac] (where Ar = Ph, or, 2,6-diisopropylphenyl), KO<sup>t</sup>Bu, and Pd(PhCN)<sub>2</sub>Cl<sub>2</sub> at a 1:1:1 M ratio in methanol produces the previously synthesized [Pd(Ph<sub>2</sub>nacnac)(μ-Cl)]<sub>2</sub> (**1a**), and newly characterized [Pd(Dipp<sub>2</sub>nacnac)(μ-Cl)]<sub>2</sub> (**1b**) as green precipitates in moderate yields of 65%, and 58%, respectively (Scheme 1). An alternative palladium source that can be used is Na<sub>2</sub>PdCl<sub>4</sub> which gives approximately the same yield in the synthesis of **1a**, but a lower yield of 35% for the synthesis of **1b**.

When the synthesis of [Pd(Ar<sup>F</sup><sub>2</sub>nacnac)(μ-Cl)]<sub>2</sub> (**1c**) (where Ar<sup>F</sup> = 3,5-bis(trifluoromethyl)phenyl) was carried out by mixing H[Ar<sup>F</sup><sub>2</sub>nacnac], KO<sup>t</sup>Bu, and Na<sub>2</sub>PdCl<sub>4</sub> at a 1:1:1 M ratio in methanol, a dark brown precipitate resulted after overnight. <sup>1</sup>H, and <sup>19</sup>F NMR spectra of the crude brown precipitate revealed the presence of two symmetrical species in a 2:5 ratio; this was indicated in the <sup>1</sup>H NMR spectrum by the presence of two singlets at 5.61 and 5.00 ppm which were tentatively assigned as the β-CH, and two singlets at 1.86 and 1.62 ppm which were tentatively assigned as the nacnac backbone methyl signals, and two singlets in the <sup>19</sup>F NMR spectrum at -64.55 and -64.26 ppm. Leaving a CH<sub>2</sub>Cl<sub>2</sub> solution of the brown crude to slowly evaporate lead to the observation of two distinct types of crystals which were green and red. The



**Scheme 1.** Synthesis of [Pd(Ph<sub>2</sub>nacnac)(μ-Cl)]<sub>2</sub> (**1a**) previously reported [6] and [Pd(Dipp<sub>2</sub>nacnac)(μ-Cl)]<sub>2</sub> (**1b**), where Dipp = 2,6-diisopropylphenyl.



**Scheme 2.** Synthesis of [Pd(Ar<sup>F</sup><sub>2</sub>nacnac)(μ-Cl)]<sub>2</sub> (**1c**) and [Pd(Ar<sup>F</sup><sub>2</sub>nacnac)<sub>2</sub>] (**2**), where Ar<sup>F</sup> = 3,5-bis(trifluoromethyl)phenyl.

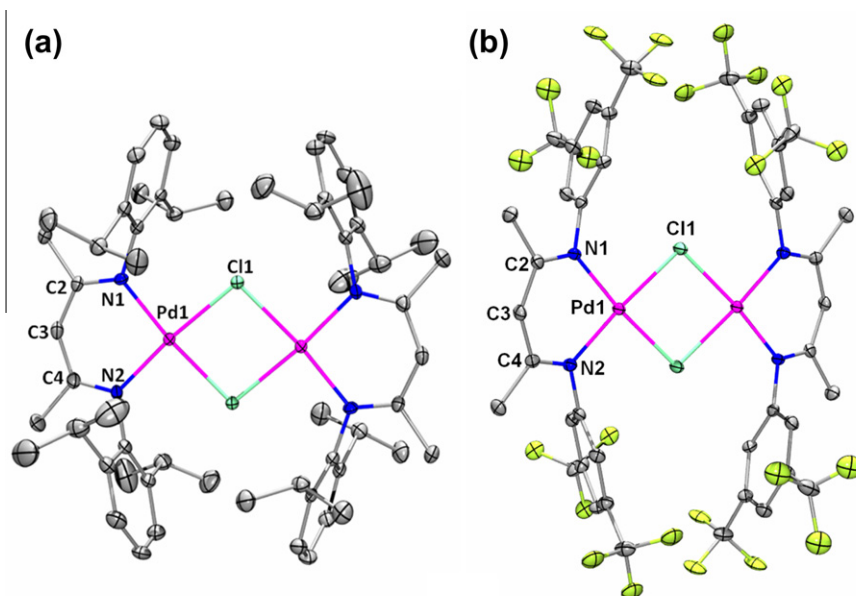


**Fig. 2.** Molecular structures of **1b** (a) and **1c** (b) with 30% probability ellipsoids. Hydrogen atoms are omitted for clarity. Selected bond lengths (Å) and angles (°) for **1b**: Pd1–N1, 2.013(3); Pd1–N2, 2.023(2); Pd1–Cl1, 2.3538(11); N1–Pd1–N2, 91.77(10); N1–Pd1–Cl1, 94.29(7); N2–Pd1–Cl1A, 93.68(7). Selected bond lengths (Å) and angles (°) for **1c**: Pd1–N2, 1.989(4); Pd1–N1, 2.005(4); Pd1–Cl1, 2.3498(14); N2–Pd1–N1, 90.95(17); N1–Pd1–Cl1, 94.20(13); N2–Pd1–Cl1A, 92.41(12).

red crystals seemed to also form faster than the green ones, and also more near the bottom of the recrystallization vial. After a series of recrystallizations (see Section 2 for details) the green, and red crystals could be cleanly separated; X-ray crystallography revealed that the green crystals were of  $[\text{Pd}(\text{Ar}^{\text{F}_2}\text{nacnac})(\mu\text{-Cl})_2]$  (**1c**), and the red crystals were of  $[\text{Pd}(\text{Ar}^{\text{F}_2}\text{nacnac})_2]$  (**2**); satisfactory elemental analysis results were obtained. The yields of **1c** and **2** were 25% and 6%, respectively (Scheme 2).

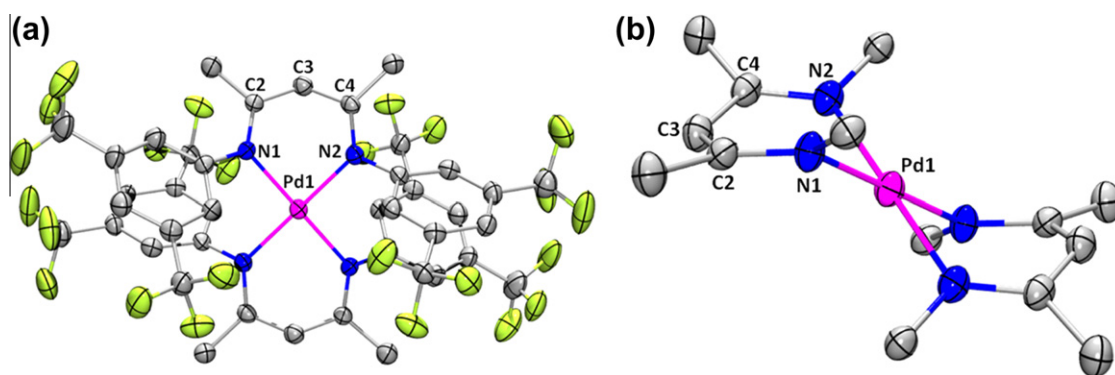
All three  $[\text{Pd}(\text{Ar}_2\text{nacnac})(\mu\text{-Cl})_2]$  complexes **1a** [6], **1b**, and **1c** are green and air- and moisture-stable both in the solid state, and in solution as monitored by NMR spectroscopy over a few days. They tend to be very soluble in most common organic solvents such as chloroform, dichloromethane, THF, diethyl ether, benzene, and toluene, somewhat soluble in acetone, but poorly soluble in methanol, water or hexanes and pentane.

The X-ray crystal structures of **1b** and **1c** are shown in Fig. 2. All three **1a** [6], **1b**, **1c** crystallize in the monoclinic space group  $P2_1/n$  with a crystallographically imposed inversion centre in the middle of the molecule. In the structure of **1c** the trifluoromethyl groups are disordered over two positions and there is also a disordered  $\text{CH}_2\text{Cl}_2$  solvent molecule. The Pd(II) centres in all three derivatives

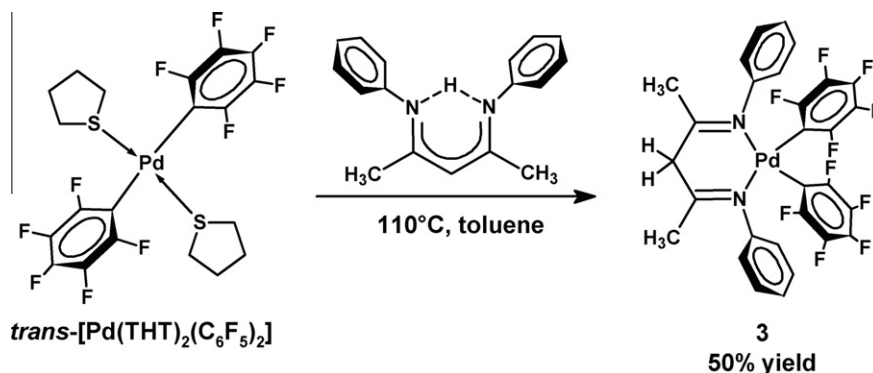
adopts a typical square-planar coordination geometry, with two N and two bridging Cl atoms occupying the four coordination sites and displaying typical bond lengths and angles. The six-membered chelate rings in all three derivatives adopt a boat conformation, folding along  $\text{N1}\cdots\text{N2}$  and  $\text{C2}\cdots\text{C4}$  axes. The dihedral angle between the planes defined by N1, Pd, N2 and C2, C3, C4 is 27° for **1a** [6], 19° for **1b**, and 26° for **1c**.

The  $^1\text{H}$  NMR spectra of **1b** and **1c** reveal the symmetrical structures of these complexes in solution giving rise to a singlet for the  $\beta\text{-CH}$ , and a singlet for the nacnac backbone methyl protons with an integration of 1:3. In  $^1\text{H}$  NMR spectrum for **1b** there are two sets of doublets corresponding to methyl protons of the *i*Pr groups suggesting hindered rotations on the NMR timescale.

The X-ray crystal structure of **2** is shown in Fig. 3. Structurally similar bis-nacnac Pd complexes characterized by X-ray crystallography in the literature are  $[\text{Pd}(\text{iPr}_2\text{nacnac})_2]$  [2], and  $[\text{Pd}(\text{Ph}_2\text{nacnac})_2]$  [20]. Complex **2** crystallizes in the monoclinic space group  $P2_1/n$ , with a crystallographically imposed inversion centre at Pd1. The six-membered chelate rings adopt a puckered conformation, folding along  $\text{N1}\cdots\text{N2}$  axis. The binding mode of  $[\text{Ar}^{\text{F}_2}\text{nacnac}]^-$ , seen clearly in Fig. 2b demonstrates that Pd is not in the



**Fig. 3.** Molecular structure of **2** (a) and an alternate side-view of **2** (b) displaying the binding mode of the two  $[\text{Ar}^{\text{F}_2}\text{nacnac}]^-$  ligands more clearly. Both views of the structure are shown with 30% probability ellipsoids. Hydrogen atoms are omitted for clarity. In b), only the *ipso*-carbons of the 3,5-bis(trifluoromethyl)phenyl groups are shown for clarity. Selected bond lengths (Å) and angles (°) for **2**: Pd1–N1, 2.027(4); Pd1–N2, 2.034(4); N1–Pd1–N2, 87.63(18).

Scheme 3. Synthesis of **3**.

ligand plane. The dihedral angle between the planes defined by N1, Pd1, N2 (the metal coordination plane) and N1, C2, C3, C4, N2 (the [Ar<sup>F</sup><sub>2</sub>nacnac]<sup>-</sup> ligand plane) is 45° for **2**. There is a change in the dihedral angle between the metal coordination plane and the nacnac ligand plane upon changing the *N,N'*-substituents from *i*Pr, to Ph, to Ar<sup>F</sup>, likely due to sterics. In [Pd(*i*Pr<sub>2</sub>nacnac)<sub>2</sub>] the aforementioned dihedral angle is 54° [2], and in [Pd(Ph<sub>2</sub>nacnac)<sub>2</sub>] the angle is 50° [20].

### 3.2. Synthesis of [Pd((PhN=C(CH<sub>3</sub>)<sub>2</sub>)<sub>2</sub>CH<sub>2</sub>)(C<sub>6</sub>F<sub>5</sub>)<sub>2</sub>] (**3**)

In an attempt to synthesize [Pd(Ph<sub>2</sub>nacnac)(C<sub>6</sub>F<sub>5</sub>)(THT)] (where THT = tetrahydrothiophene), which would provide a <sup>19</sup>F NMR spectroscopic handle to study insertion/polymerization reactivity we isolated a palladium(II) β-diimine complex **3**. Refluxing *trans*-Pd(THT)<sub>2</sub>(C<sub>6</sub>F<sub>5</sub>)<sub>2</sub> with H[Ph<sub>2</sub>nacnac] in toluene (Scheme 3) gave a pale yellow solution with some Pd black. After filtration to remove the Pd black and concentration of the filtrate a white microcrystalline powder of **3** can be precipitated out upon the addition of hexanes in 50% yield. X-ray diffraction quality crystals can be grown from a CH<sub>2</sub>Cl<sub>2</sub>-MeOH solvent mixture at -30 °C (Fig. 4). The <sup>1</sup>H NMR spectrum reflects the symmetrical nature of **3** giving rise to a singlet at 4.46 ppm corresponding to the β-CH<sub>2</sub>, and a singlet at 2.30 ppm corresponding to the methyl protons of the β-diimine backbone, the <sup>19</sup>F NMR spectrum has three sets of peaks corresponding to the *ortho*-, *meta*- and *para*- fluorines.

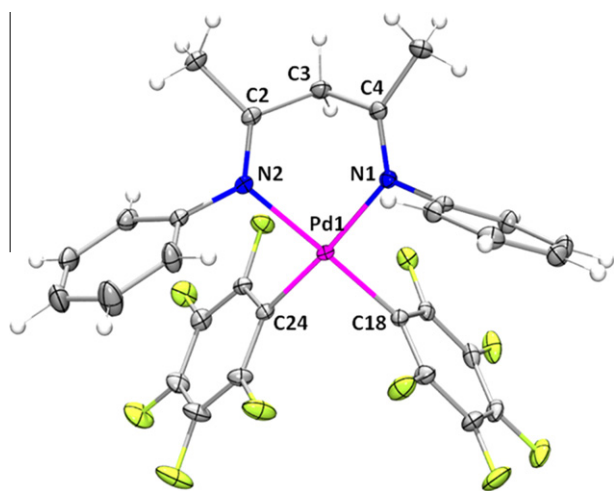
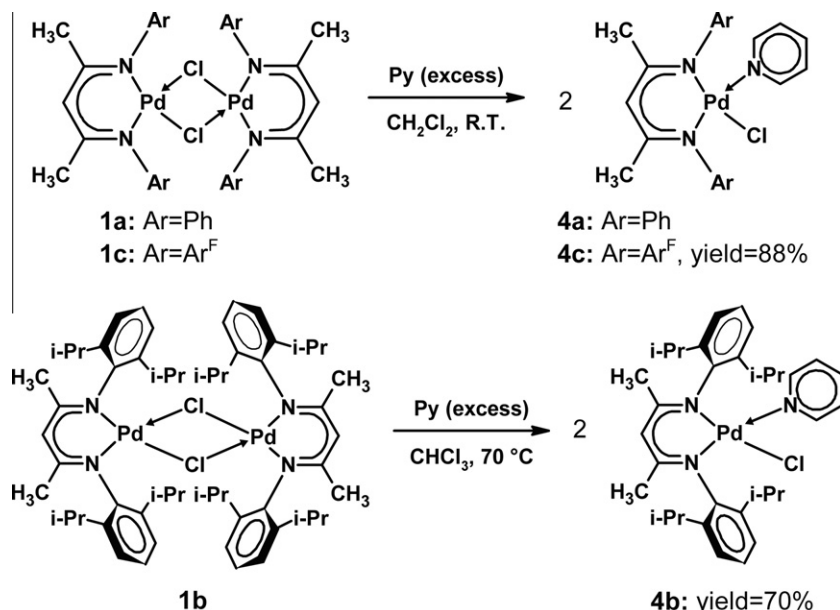


**Fig. 4.** Molecular structure of **3** with 30% probability ellipsoids. Hydrogen atoms are shown as spheres of arbitrary radius. Selected bond lengths (Å) and angles (°) for **3**: Pd1–N1, 2.0941(16); Pd1–N2, 2.0872(16); Pd1–C18, 2.0050(19); Pd1–C24, 2.0037(19); N2–Pd1–N1, 86.59(6); C24–Pd1–C18, 87.12(8); C24–Pd1–N2, 90.23(7); C18–Pd1–N1, 95.94(7).

The X-ray crystal structure of **3** is shown in Fig. 4, where the Pd centre displays a typical square planar geometry with two *cis*-N and two *cis*-C donor atoms occupying the four coordination sites and displaying typical bond lengths and angles. Complex **3** crystallizes in monoclinic space group *P*2<sub>1</sub>/*n*. The six-membered chelate ring adopts a boat conformation, folding along N1···N2 and C2···C4 axes. The dihedral angle between the planes defined by N1, Pd, N2 and C2, C3, C4 is 86.43°.

Usually *cis*-diarylpalladium complexes are difficult to isolate because of facile reductive elimination of biaryl compounds from the complex. Complex **3** is quite thermally stable, also it is air- and moisture-stable in the solid state and in solution, likely because the Pd–C(sp<sup>2</sup>) bonds are strengthened by fluorine substitution. This also has implications for palladium catalyzed C–C coupling reactions which typically involve [(L)Pd(Ar)(Ar')] intermediates, if both Ar and Ar' are electron-withdrawing the reductive elimination is usually extremely slow/infrequent resulting in low yields of biaryl product. Several stable *cis*-[Pd(C<sub>6</sub>F<sub>5</sub>)<sub>2</sub>(L')] (where L' is a neutral bidentate ligand) complexes have been characterized [13,21–23].

Yamamoto and coworkers found that reductive elimination could be promoted from complexes of the form *cis*-[Pd(C<sub>6</sub>F<sub>5</sub>)<sub>2</sub>(L')] to form (C<sub>6</sub>F<sub>5</sub>)–(C<sub>6</sub>F<sub>5</sub>) upon the addition of acid, where the trend in efficiency of this process seemed to be dependent on a few structural parameters such as Pd–C<sub>ipso</sub> bond length, C<sub>ipso</sub>–C<sub>ipso</sub> distance, the C<sub>ipso</sub>–Pd–C<sub>ipso</sub> angle, and dihedral angle between the two planes of the C<sub>6</sub>F<sub>5</sub> rings [23]. Generally, the longer Pd–C<sub>ipso</sub> bond length, the shorter the C<sub>ipso</sub>–C<sub>ipso</sub> distance, the narrower the C<sub>ipso</sub>–Pd–C<sub>ipso</sub> angle, and the more acute the dihedral angle between the two C<sub>6</sub>F<sub>5</sub> planes, the more facile the reductive elimination to form (C<sub>6</sub>F<sub>5</sub>)–(C<sub>6</sub>F<sub>5</sub>) was. The values for the aforementioned structural parameters in complex **3** are as follows (distances in Å, angles in °); Pd1–C18: 2.0050(19), Pd1–C24: 2.0037(19), C18–C24: 2.762, C18–Pd1–C24: 87.12(8), plane(C<sub>6</sub>F<sub>5</sub>)–plane(C<sub>6</sub>F<sub>5</sub>): 84.56. The Pd–C<sub>ipso</sub> bonds in **3** are relatively short as compared with either [Pd(C<sub>6</sub>F<sub>5</sub>)<sub>2</sub>(cod)] (2.032(4)), [Pd(C<sub>6</sub>F<sub>5</sub>)<sub>2</sub>(bpy)] (2.009(6)(*av.*)), [Pd(C<sub>6</sub>F<sub>5</sub>)<sub>2</sub>(dppe)] (2.087(2)(*av.*)), [Pd(C<sub>6</sub>F<sub>5</sub>)<sub>2</sub>(dppb)] (2.062(4)) [23]. The C<sub>ipso</sub>–C<sub>ipso</sub> distance is relatively short as compared with either [Pd(C<sub>6</sub>F<sub>5</sub>)<sub>2</sub>(cod)] (2.842(6)), [Pd(C<sub>6</sub>F<sub>5</sub>)<sub>2</sub>(bpy)] (2.747(8)), [Pd(C<sub>6</sub>F<sub>5</sub>)<sub>2</sub>(dppe)] (3.026(3)), [Pd(C<sub>6</sub>F<sub>5</sub>)<sub>2</sub>(dppb)] (2.829(5)) [23]. The C<sub>ipso</sub>–Pd–C<sub>ipso</sub> angle in **3** is intermediate when compared with either [Pd(C<sub>6</sub>F<sub>5</sub>)<sub>2</sub>(cod)] (88.75(19)), [Pd(C<sub>6</sub>F<sub>5</sub>)<sub>2</sub>(bpy)] (86.3(2)), [Pd(C<sub>6</sub>F<sub>5</sub>)<sub>2</sub>(dppe)] (92.90(8)), [Pd(C<sub>6</sub>F<sub>5</sub>)<sub>2</sub>(dppb)] (86.65(16)) [23]. Finally the dihedral angle between the two C<sub>6</sub>F<sub>5</sub> planes in **3** is relatively acute as compared with either [Pd(C<sub>6</sub>F<sub>5</sub>)<sub>2</sub>(cod)] (88.9), [Pd(C<sub>6</sub>F<sub>5</sub>)<sub>2</sub>(bpy)] (89.9), [Pd(C<sub>6</sub>F<sub>5</sub>)<sub>2</sub>(dppe)] (104.1), [Pd(C<sub>6</sub>F<sub>5</sub>)<sub>2</sub>(dppb)] (86.6) [23]. Yamamoto and co-workers found that reductive elimination from [Pd(C<sub>6</sub>F<sub>5</sub>)<sub>2</sub>(cod)] and [Pd(C<sub>6</sub>F<sub>5</sub>)<sub>2</sub>(dppb)] upon the addition of HNO<sub>3</sub> selectively gave reductive elimination of (C<sub>6</sub>F<sub>5</sub>)–(C<sub>6</sub>F<sub>5</sub>), while



**Scheme 4.** Cleavage of  $[\text{Pd}(\text{Ar}_2\text{nacnac})(\mu\text{-Cl})_2]$  (**1**) by pyridine (Py).

$[\text{Pd}(\text{C}_6\text{F}_5)_2(\text{bpy})]$  gave only a very low yield of biaryl after extended period of time, and  $[\text{Pd}(\text{C}_6\text{F}_5)_2(\text{dppe})]$  gave the protonolysis product  $\text{HC}_6\text{F}_5$  [23].

### 3.3. Reactivity of $[\text{Pd}(\text{Ar}_2\text{nacnac})(\mu\text{-Cl})_2]$ towards neutral monodentate ligands

$[\text{Pd}(\text{Ph}_2\text{nacnac})(\mu\text{-Cl})_2]$  (**1a**) has been shown previously to be an excellent starting material for the preparation of mononuclear species of the form  $[\text{Pd}(\text{Ph}_2\text{nacnac})(\text{L})\text{Cl}]$ . When neutral monodentate ligands (L) such as CO [6], *N*-methyl-4,5-diphenylimidazole (L2) [6], 4-*t*-butylaniline [6,7], and pyridine [8] are added the chloride bridge breaks. Complex **1a** reacts with CO to form  $[\text{Pd}(\text{Ph}_2\text{nacnac})(\text{CO})\text{Cl}]$  which is only stable under an atmosphere of CO; even in the solid-state wet crystals  $[\text{Pd}(\text{Ph}_2\text{nacnac})(\text{CO})\text{Cl}]$  can lose CO to reform complex **1a** [6]. When CO is bubbled through a  $\text{CDCl}_3$  solution of **1b** there is no apparent change by NMR spectroscopy and the solution remains a dark green colour. Apparently the bulky Dipph groups of **1b** seem to inhibit dimer cleavage by CO.

Complexes **1a** and **1c** react rapidly upon mixing at room temperature with pyridine in  $\text{CH}_2\text{Cl}_2$  to form the previously characterized complex **4a** [8], and **4c**, respectively which can be isolated as red–orange crystals (Scheme 4). However simply reacting **1b** with excess pyridine at room temperature does not give any reaction even after 1 h. In order to cleave the chloride bridges in complex **1b** excess pyridine and elevated temperatures of 70 °C for 3 h are required to form **4b** (Scheme 4).

$^1\text{H}$  NMR spectra for either **4b** or **4c** reflects the fact that the two nacnac backbone methyl groups are inequivalent; for complex **4b** these resonances appear at 1.70 and 1.66 ppm, and for complex **4c** these appear at 1.73 and 1.72 ppm. Fig. 5 depicts the X-ray crystal structures of **4b** and **4c**, in both of the complexes the Pd centre adopts a typical square planar geometry and is coordinated to two N-donors from the nacnac ligand in a *cis*-fashion, one terminal Cl, and an N-donor atom from pyridine to occupy the four coordination sites. Complex **4b** crystallizes in the triclinic space group  $P\bar{1}$ , and complex **4c** crystallizes in the monoclinic space group  $P2_1/n$  with half a molecule of disordered  $\text{CH}_2\text{Cl}_2$  per each molecule of **4c**. The trifluoromethyl groups in complex **4c** are disordered over two positions.

The six-membered chelate ring in complex **4a** was reported as having a puckered conformation where dihedral angle between the N1, Pd, N2 and C2, C3, C4 planes was 19.78° [8]. The six-membered chelate ring in complex **4b** adopts an almost planar conformation, but does fold slightly along N1...N2 axis, and the dihedral angle between the N1, Pd, N2 and C2, C3, C4 planes is only 13.94°. The six-membered chelate ring in complex **4b** adopts a puckered conformation, folding along N1...N2 axis, the dihedral angle between the N1, Pd, N2 and C2, C3, C4 planes is 37.39°.

### 3.4. Metal–ligand co-operative dioxygen activation in a Pd nacnac complex

When a  $\text{CH}_2\text{Cl}_2$  solution of **1b** and 2 equivalents of 1-methylimidazole (Me-Im) was left in air for 2 months red crystals were obtained of complex  $[\text{Pd}(\mathbf{L1})\text{Cl}(\text{Me-Im})]$  (**5**) (Scheme 5). In the process of generating complex **5**, the chloride bridge has been cleaved, and the backbone  $\beta\text{-C}$  activated dioxygen to form an *N,O*-chelate chelating ligand ( $\mathbf{L1}^-$ ) which forms a 5-membered chelate ring with Pd. The synthesis of complex **5** is an example of the non-innocent and reactive nature of the  $\beta\text{-C}$  in nacnac ligands, a recurring theme in the chemistry of this ligand set. Examples for the reactivity of the  $\beta\text{-C}$  towards dioxygen in transition metal nacnac complexes are known [24–26]. Itoh and co-workers reported Cu(II) and Zn(II) complexes of  $[\text{Mes}_2\text{nacnac}]^-$  (where Mes is mesityl) ligand that easily underwent an oxidative degradation to afford a ketone diimine where the backbone  $\beta\text{-C}$  had been oxidized to a carbonyl [24]. An *N,O*-chelate ligand very similar to  $\mathbf{L1}^-$  has been seen on Cu(II) where the aryl groups on N are either Mes [24], or Dipph [25], where the main difference is that the dioxygen-derived functional group is a hemiacetal. Itoh and coworkers had suggested [24], and Goldberg and co-workers have demonstrated [26] that a “metal–O–O–C” peroxo intermediate might be involved in the oxidation of nacnac to a ketone diimine. Goldberg and co-workers have isolated a Pt(IV) complex with a ligand similar to  $\mathbf{L1}^-$  generated from dioxygen activation where the ligand acts as a tridentate *N,O,N*-donor ligand to  $\{\text{Pt}(\text{Me})_3\}^+$  cation [26].

The crystal structure of complex **5** is shown in Fig. 6. The Pd(II) centre adopts a typical square-planar coordination geometry, with two *cis*-coordination sites occupied by the *N,O* chelate **L1**, a Cl

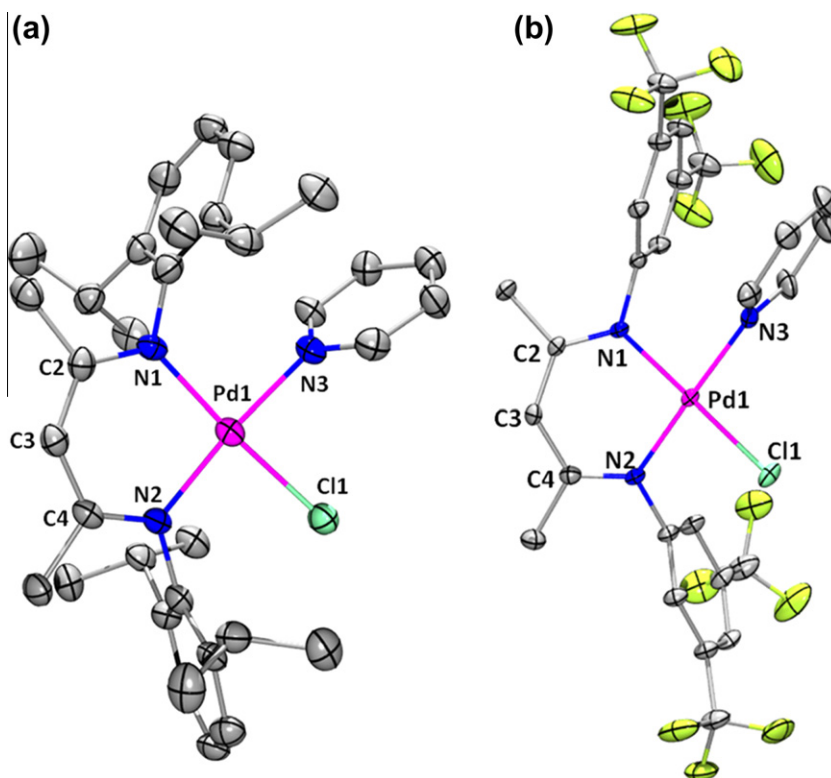


**Fig. 5.** Molecular structures of **4b** (a) and **4c** (b) with 30% probability ellipsoids. Hydrogen atoms are omitted for clarity. Selected bond lengths (Å) and angles (°) for **4b**: Pd1–N1, 2.031(11); Pd1–N2, 2.014(10); Pd1–N3, 2.078(10); Pd1–Cl1, 2.314(4); N2–Pd1–N1, 91.7(4); N3–Pd1–Cl1, 82.0(3); N1–Pd1–N3, 94.3(4); N2–Pd1–Cl1, 92.0(3). Selected bond lengths (Å) and angles (°) for **4c**: Pd1–N1, 2.027(3); Pd1–N2, 2.005(4); Pd1–N3, 2.040(4); Pd1–Cl1, 2.3165(11); N2–Pd1–N1, 89.71(14); N3–Pd1–Cl1, 86.96(11); N1–Pd1–N3, 91.43(14); N2–Pd1–Cl1, 91.98(10).

atom, and N-atom from Me-Im occupying the four coordination sites, and displaying typical bond lengths and angles. The  $^1\text{H}$  NMR spectrum shows that all four  $-\text{CH}(\text{Me})_2$  are inequivalent, four septets were observed at 3.60, 3.48, 3.25, and 2.79 ppm.

Unfortunately the synthesis of complex **5** has poor reproducibility and only an X-ray crystal structure, and  $^1\text{H}$  NMR spectrum was obtained.

### 3.5. Synthesis and characterization of $[\text{Pd}(\text{Ph}_2\text{nacnac})\text{L}_2]^+$ cationic complexes

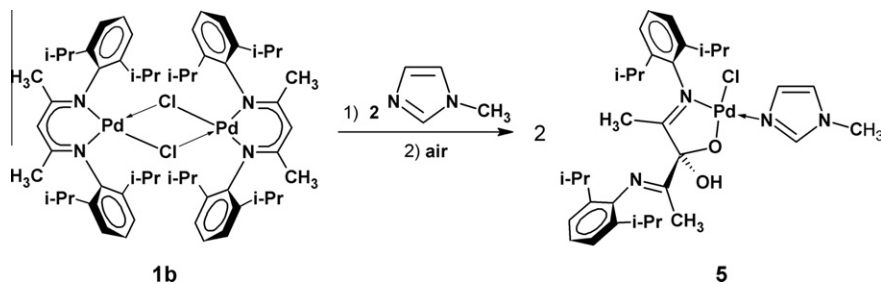
The reaction of **1a** with neutral and monodentate L-type ligands can be further expanded to produce complexes of the form  $[\text{Pd}(\text{Ph}_2\text{nacnac})\text{L}_2]\text{BF}_4$  (Scheme 6). Reaction of **1a** under argon with four equivalents of a L-type ligand, such as *N*-methyl-4,5-diphenylimidazole (**L2**), and two equivalents of  $\text{NaBF}_4$  results in chloride abstraction and the formation of  $[\text{Pd}(\text{Ph}_2\text{nacnac})(\text{L2})_2]\text{BF}_4$  (**6**).

Complex **6** crystallized in the monoclinic space group  $P2_1/c$  (Fig. 7). The Pd(II) centre is square-planar with all four coordination sites occupied by nitrogen atoms. The Pd1–N1 and Pd1–N2

bond distances are 2.005(3) Å and 1.998(3) Å, respectively, and the Pd–Ph<sub>2</sub>nacnac ring adopts a boat conformation, with a dihedral angle between the N1, Pd1, N2 and C2, C3, C4 planes of  $\sim 49^\circ$ . The conformation that the ring adopts (planar or boat) seems to depend on the nature of the ligands around the Pd centre. Boat conformations are generally seen in  $[\text{Pd}(\text{Ar}_2\text{nacnac})(\mu\text{-Cl})_2]$  and in complexes where there is a bond or interaction at the  $\beta\text{-C}$  of the nacnac backbone [4,6–8], whereas a planar conformation was seen in  $[\text{Pd}(\text{Ph}_2\text{nacnac})\text{Cl}(\text{L2})]$  [6]. The imidazole rings in **6** have their methyl groups pointing in opposite directions. The imidazole methyl protons (5.39 ppm) are shifted significantly upfield from that of  $[\text{Pd}(\text{Ph}_2\text{nacnac})\text{Cl}(\text{L2})]$  (7.26 ppm), most likely due to their positioning with respect to the phenyl groups on imidazole, resulting in a ring current effect.

### 3.6. Unusual transmetalation-induced formation of a $C_2$ -symmetric tetrapallada-macrocycles and reactivity

Recently we discovered a rather surprising example of transmetalation when phenylboronic acid is used as the



**Scheme 5.** Synthesis of **5**.

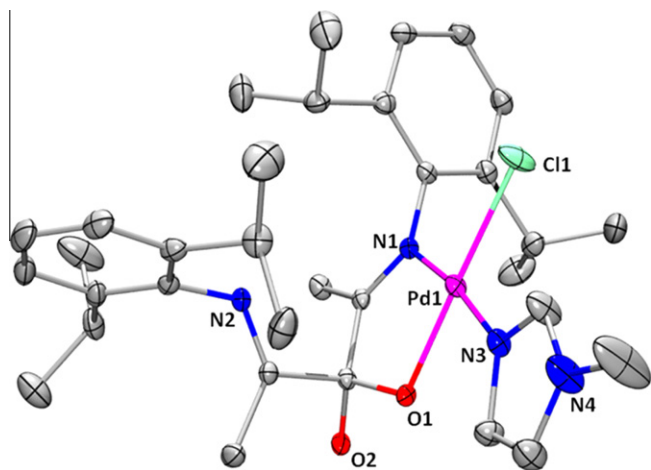


**Fig. 6.** Molecular structure of O<sub>2</sub>-activation product **5** with 30% probability ellipsoids. Hydrogen atoms are omitted for clarity. Selected bond lengths (Å) and angles (°) for **5**: Pd1–O1, 2.0031(16); Pd1–N1, 2.021(2); Pd1–N3, 2.022(2); Pd1–Cl1, 2.2814(9); O1–Pd1–N1, 82.15(8); N3–Pd1–Cl1, 91.83(7); O1–Pd1–N3, 90.11(8); N1–Pd1–Cl1, 95.91(6).

transmetallation reagent to synthesize the C<sub>2</sub>-symmetric tetrapal-lada-macrocyclic complex **7a** [8]. This transmetallation reaction is unusual since an anionic bidentate chelate ligand is replaced by a phenyl ligand from phenylboronic acid, leaving the chloride ligands intact. As shown in Scheme 7, when a mixture of **1a** and 1.3 equiv. of an arylboronic acid (where Ar = Ph, or 4-fluorophenyl) in a wet benzene/acetone solvent mixture is heated at 75 °C, with in hours orange X-ray diffraction quality single crystals of analytically pure **7a**, and **7b** can be isolated in ~50% yield. Both **7a** and **7b** are slightly soluble in dichloromethane and 1,2-dichloroethane, but insoluble in benzene, acetone, hexanes, diethyl ether, THF, methanol, water, chloroform and DMSO. Interestingly **1b** and **1c** do not react at all with arylboronic acids.

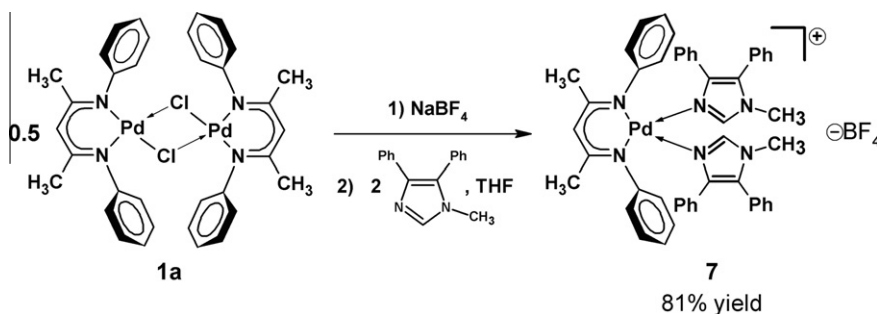
The X-ray crystal structure of **7b** is shown in Fig. 8, and is very similar to that of **7a** [8], both crystallize in the monoclinic space group C<sub>2/c</sub> with a C<sub>2</sub> axis running down the centre of the molecule. The structure can be viewed as two {(4-FPh)Pd(μ-Cl)<sub>2</sub>Pd(Ph<sub>2</sub>nacnac)} units assembled via two Pd–C (the central backbone β-carbon of [Ph<sub>2</sub>nacnac]<sup>−</sup> ligand) bonds. Each [Ph<sub>2</sub>nacnac]<sup>−</sup> ligand in **7b** uses two N-donors to chelate to a Pd center in one {(4-FPh)Pd(μ-Cl)<sub>2</sub>Pd(Ph<sub>2</sub>nacnac)} unit, while the sp<sup>3</sup> hybridized β-carbon coordinates to a Pd center in the other unit. The six-membered chelate ring comprised of the {(Ph<sub>2</sub>nacnac)Pd} moiety adopts a boat conformation. A similar coordination mode for [Ar<sub>2</sub>nacnac]<sup>−</sup> has also been reported by Feldman and co-workers in a dinuclear tricationic Pd(II) complex [4], and our group in an unusual trinuclear Pd(II)–Ph<sub>2</sub>nacnac complex with amido-chloro double-bridges [7]. The Pd<sub>2</sub>–C3A bond length in **7b** is 2.103(3) Å, similar to **7a** (2.099(3) Å) [8], and

to other literature values for Pd–(β-C) bond lengths [4,7]. The *ipso*-carbon of the phenyl ligand and the β-carbon donor of the [Ph<sub>2</sub>nacnac]<sup>−</sup> ligand are mutually *cis*- and the coordination environment around each Pd(II) center is square planar. The two methyl groups of each [Ph<sub>2</sub>nacnac]<sup>−</sup> ligand are no longer equivalent: the methyl group containing C5 (Fig. 8) is situated in the shielding region of a phenyl ligand, while the methyl group containing C1 has no phenyl ligand nearby. Accordingly, the two singlets at 2.07, and 0.95 ppm in the <sup>1</sup>H NMR spectrum of **7b** can be assigned to the two methyl groups containing C1 and C5, respectively.

We decided to probe the reactivity of **7a** towards L-type ligands in an attempt to force the reductive coupling of the mutually *cis*-phenyl ligand and [Ph<sub>2</sub>nacnac]<sup>−</sup> ligand. Similar to complex **1a**, complex **7a** possesses bridging chlorides. When complex **7a** is treated with 6 equiv. of pyridine the chloride bridges are cleaved, in addition the Pd–(β-C) bond is cleaved and in the process two equivalents of **4a** and two equivalents of *trans*-[Pd(Py)<sub>2</sub>(Ph)Cl] form as monitored by <sup>1</sup>H NMR spectroscopy (Scheme 8). The NMR data of both **4a** [8], and *trans*-[Pd(Py)<sub>2</sub>(Ph)Cl] [19] are reported previously. Furthermore, recrystallization of reaction mixture from CH<sub>2</sub>Cl<sub>2</sub>–hexanes gave both orange crystals of **4a**, and colourless crystals of *trans*-[Pd(Py)<sub>2</sub>(Ph)Cl]. The synthesis and NMR characterization of *trans*-[Pd(Py)<sub>2</sub>(Ph)Cl] has been reported in the literature [19], here we report the X-ray crystal structure of this simple coordination complex that crystallized in the monoclinic space group C<sub>2/c</sub> (see Fig. 9). The addition of 1 equiv. of pyridine at a time in an attempt to pinpoint which bond is cleaved first only showed incomplete conversion to **4a** and *trans*-[Pd(Py)<sub>2</sub>(Ph)Cl].

### 3.7. Pyridine abstraction from **4a** by boronic acids

The unusual transmetallation reaction observed between **1a** and boronic acids to form either complex **7a** or **7b** prompted us to investigate whether the fact that **1a** possesses bridging chlorides as opposed to terminal chlorides might be the reason. Previously we showed that when complex **4a**, which possesses a terminal chloride, is treated with MeLi the conventional [27] transmetallation product [Pd(Ph<sub>2</sub>nacnac)(Py)(Me)] was isolated and characterized [8]. When complex **4a** is treated with 1.2 equiv. of phenylboronic acid in dry C<sub>6</sub>D<sub>6</sub>, an equilibrium is established between the starting material **4a**, and [Pd(Ph<sub>2</sub>nacnac)Cl]<sub>2</sub> (**1a**) the product of pyridine abstraction by phenylboronic acid (Scheme 9). The addition of an excess of phenylboronic acid to **4a** pushes the equilibrium towards the formation [Pd(Ph<sub>2</sub>nacnac)Cl]<sub>2</sub> (see Supporting Information for NMR spectra where 2.5 and 5 equiv. of phenylboronic acid was added). Pyridine abstraction from a transition metal complex by 3-coordinate Lewis acidic boranes, such as B(C<sub>6</sub>F<sub>5</sub>)<sub>3</sub>, has been employed several times in the past, and in the process of generating catalytically active species for olefin polymerization [28,29]. To the best of our knowledge this



**Scheme 6.** Synthesis of **6**.

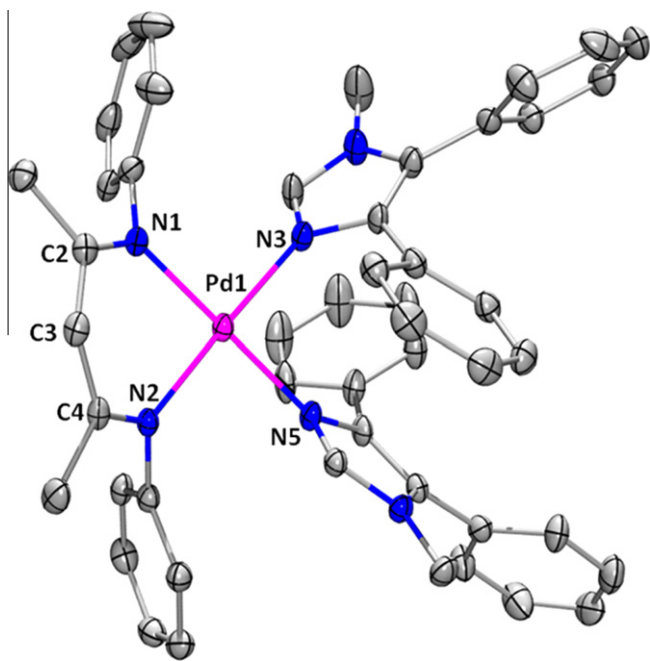
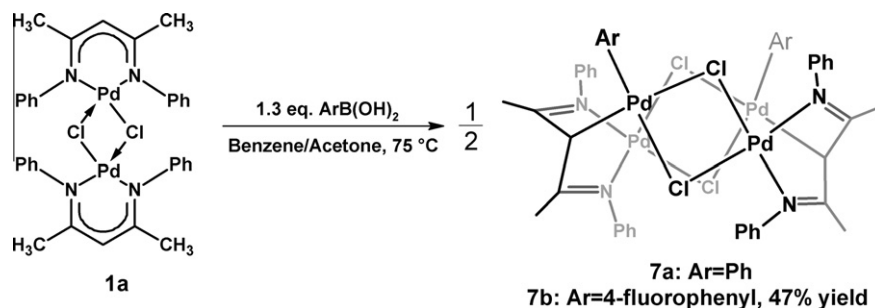


**Fig. 7.** Molecular structure of **6** with 30% probability ellipsoids. The counteranion and hydrogen atoms are omitted for clarity. Selected bond lengths (Å) and angles (°) for **6**: Pd1–N1, 2.005(3); Pd1–N2, 1.998(3); Pd1–N3, 2.032(3); Pd1–N5, 2.058(3); N2–Pd1–N1, 88.27(12); N3–Pd1–N5, 88.21(12); N1–Pd1–N3, 89.60(12); N2–Pd1–N5, 93.78(12).

represents the first example of pyridine abstraction from a transition metal complex with a boronic acid. In the  $^{11}\text{B}$  NMR spectrum there are two species (referenced against  $\text{KBF}_4$  dissolved in  $\text{D}_2\text{O}$  in a flame-sealed capillary), a major species given by a broad singlet at 24.67 ppm, and a minor species given by a sharp singlet at 3.60 ppm.

The minor boron-containing species at 3.60 ppm is likely a 4-coordinate borate species with  $[\text{Ph}_2\text{nacnac}]^-$ , or chloride coordinated to boron which could not be characterized, the result of a small amount of Pd black which formed in the reaction. The major species at 24.67 ppm is likely a Lewis acid–base adduct with approximately 1:3 pyridine:boronic acid stoichiometry, in line with what had been investigated by Yabroff and coworkers by elemental analysis, and Snyder and coworkers by IR [30–32].  $^{11}\text{B}$  NMR spectroscopy (externally referenced with  $\text{KBF}_4$ ) was conducted on mixtures of pyridine and phenylboronic acid at different stoichiometric ratios in  $\text{C}_6\text{D}_6$  under dry/inert atmosphere. It was determined that the somewhere between 0.25 equiv. of Py per phenylboronic acid ( $^{11}\text{B}$  NMR, 25.67 ppm) and 0.33 equiv. of Py ( $^{11}\text{B}$  NMR, 22.7 ppm) lies the stoichiometry of the resulting Lewis acid–base complex. The broadness of the peak at 24.67 ppm implies that there is dynamic solution behaviour in this complex.



**Scheme 7.** Synthesis of  $[(\text{Ph})\text{Pd}(\mu\text{-Cl})_2\text{Pd}(\text{Ph}_2\text{nacnac})_2]$  (**7a**) which was previously reported,[8] and the synthesis of  $[(4\text{-FPh})\text{Pd}(\mu\text{-Cl})_2\text{Pd}(\text{Ph}_2\text{nacnac})_2]$  (**7b**).

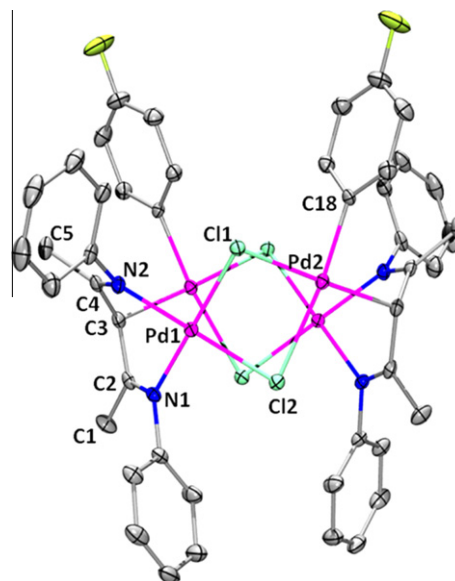
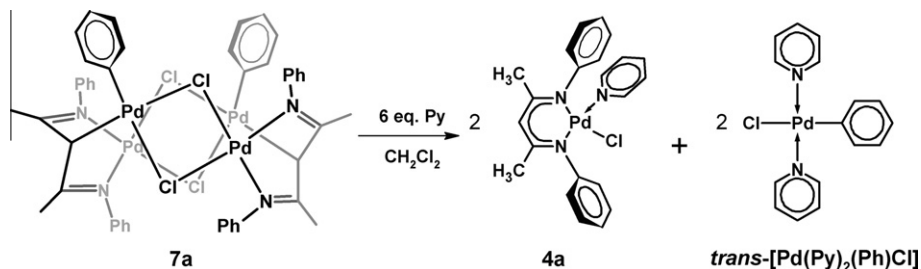


**Fig. 8.** Molecular structure of **7b** with 30% probability ellipsoids. Hydrogen atoms are omitted for clarity. Selected bond lengths (Å) and angles (°) for **7b**: Pd1–N1, 2.014(3); Pd1–N2, 1.999(3); Pd1–Cl1, 2.3363(9); Pd1–Cl2, 2.3414(9); Pd2–Cl1, 2.3911(9); Pd2–Cl2, 2.4966(9); Pd2–C18, 1.991(3); Pd2–C3, 2.103(3); N2–Pd1–N1, 85.90(12); N2–Pd1–Cl1, 93.49(9); N1–Pd1–Cl2, 94.07(8); Cl1–Pd1–Cl2, 86.53(3); C18–Pd2–C3, 87.41(14); C18–Pd2–Cl1, 90.86(10); C3–Pd2–Cl2, 99.83(10); Cl1–Pd2–Cl2, 81.95(3); Pd1–Cl2–Pd2, 85.16(3); Pd1–Cl1–Pd2, 87.71(3).

### 3.8. Reactivity of pentafluorophenylboronic acid with **1a**

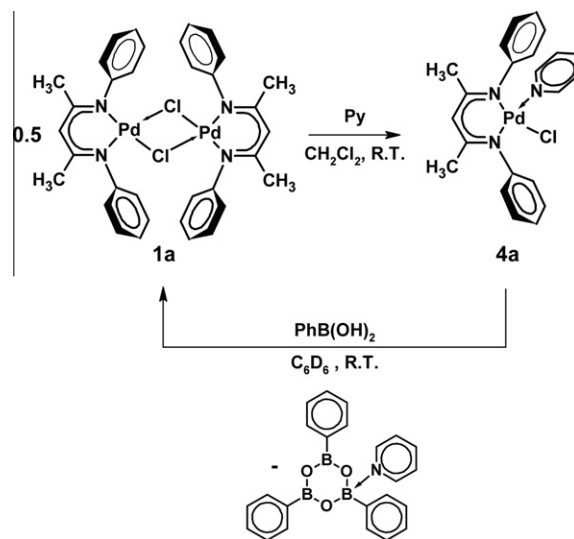
After it was observed that 4-fluorophenylboronic acid reacts with **1a** to form **7b**, it was investigated whether pentafluorophenylboronic acid could be used to form a similar tetrapalladacycle. Using similar reaction conditions as shown in Scheme 7 in a wet benzene:acetone solvent mixture the major product that was isolated out of the reaction mixture were yellow crystals of  $[\text{Pd}(\text{Ph}=\text{C}(\text{CH}_3)_2\text{CH}_2)\text{Cl}(\text{C}_6\text{F}_5)]$  (**8**). A  $\text{C}_6\text{F}_5$ -group was transferred onto Pd and the backbone  $\beta$ -C of  $[\text{Ph}_2\text{nacnac}]^-$  was protonated. The  $^1\text{H}$  NMR spectrum shows that the two  $\beta$ -diimine methyl groups were inequivalent resonating at 2.24 and 2.23 ppm, and the  $\beta$ - $\text{CH}_2$  peak at 4.60 ppm integrated for 2H relative to other peaks. The X-ray crystal structure for complex **8** is shown in Fig. 10. Compound **8** crystallized in the orthorhombic space group  $P2_12_12_1$ . Similar to complex **3** which also has the same  $\beta$ -diimine ligand and a  $-\text{C}_6\text{F}_5$  group, the six-membered chelate ring adopts a boat conformation, folding along  $\text{N1} \cdots \text{N2}$  and  $\text{C2} \cdots \text{C4}$  axes. The dihedral angle between the planes defined by N1, Pd, N2 and C2, C3, C4 is  $86.4^\circ$ . The Pd–N1 bond length is 2.029(3) Å and is shorter than the Pd–N2 bond length which is 2.119(3) Å, this observation is in agreement with the higher *trans*-influence of the  $\text{C}_6\text{F}_5$  group being



**Scheme 8.** Cleavage of chloride bridges of **7a** with pyridine yielding **4a**, and *trans*-[Pd(Py)<sub>2</sub>(Ph)Cl].

a better  $\sigma$ -donor character compared to the Cl ligand. Similar observations about the two Pd–N distances being different has been noted in other complexes of [Pd(L')(C<sub>6</sub>F<sub>5</sub>)(X)] where L' is a neutral bidentate ligand and X is either a halide or hydroxide [33,34]. Since the backbone  $\beta$ -C of [Ph<sub>2</sub>nacnac]<sup>−</sup> was protonated in order to form complex **8** from **1a** it was thought this was perhaps because the reaction was carried out in solvent which had not been dried. When the reaction of **1a** with pentafluorophenylboronic acid was carried out in dry toluene (Scheme 10) the major product isolated in 54% yield as yellow X-ray diffraction quality crystals was still complex **8**. Surprisingly, in the same reaction mixture a trace amount of red crystals had also formed at the gas-solution interface, these red crystals were of octanuclear S-shaped complex **9** (see Fig. 11).

Complex **9** crystallizes in the monoclinic space group *P*2<sub>1</sub>/*n* with a crystallographically imposed inversion centre in the middle of the molecule. The structure can be thought of as three {[Pd(Ph<sub>2</sub>nacnac)( $\mu$ -Cl)]<sub>2</sub>} units with two {Pd(C<sub>6</sub>F<sub>5</sub>)Cl} units sandwiched in between, the two outer {[Pd(Ph<sub>2</sub>nacnac)( $\mu$ -Cl)]<sub>2</sub>} units are bound to one {Pd(C<sub>6</sub>F<sub>5</sub>)Cl} unit each through one of its  $\beta$ -carbons, while the central {[Pd(Ph<sub>2</sub>nacnac)( $\mu$ -Cl)]<sub>2</sub>} unit is bound to both {Pd(C<sub>6</sub>F<sub>5</sub>)Cl} units through both of its  $\beta$ -carbons. The –C<sub>6</sub>F<sub>5</sub> groups all point inward. Each Pd centre is square planar, where similar to **1a** in the {[Pd(Ph<sub>2</sub>nacnac)( $\mu$ -Cl)]<sub>2</sub>} fragments there are two N and two bridging Cl atoms occupying the four coordination sites, while the in the {Pd(C<sub>6</sub>F<sub>5</sub>)Cl} fragment, the C-donor from C<sub>6</sub>F<sub>5</sub> and



**Scheme 9.** Pyridine abstraction from [Pd(Ph<sub>2</sub>nacnac)(Py)Cl] (**4a**) to form **1a** with PhB(OH)<sub>2</sub>.

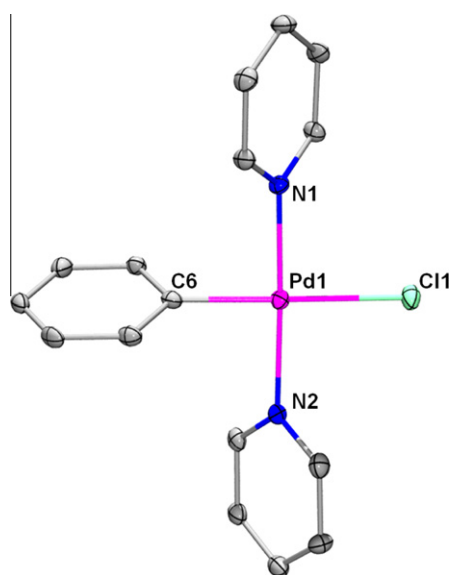


**Fig. 9.** Molecular structure of *trans*-[Pd(Py)<sub>2</sub>(Ph)Cl] with 30% probability ellipsoids. Hydrogen atoms are omitted for clarity. Selected bond lengths (Å) and angles (°) for *trans*-[Pd(Py)<sub>2</sub>(Ph)Cl]: Pd1–C6, 1.990(5); Pd1–N1, 2.049(4); Pd1–N2, 2.036(4); Pd1–Cl1, 2.4188(11); C6–Pd1–N1, 88.86(16); C6–Pd1–N2, 89.07(16); N1–Pd1–Cl1, 91.17(11); N2–Pd1–Cl1, 91.11(11).

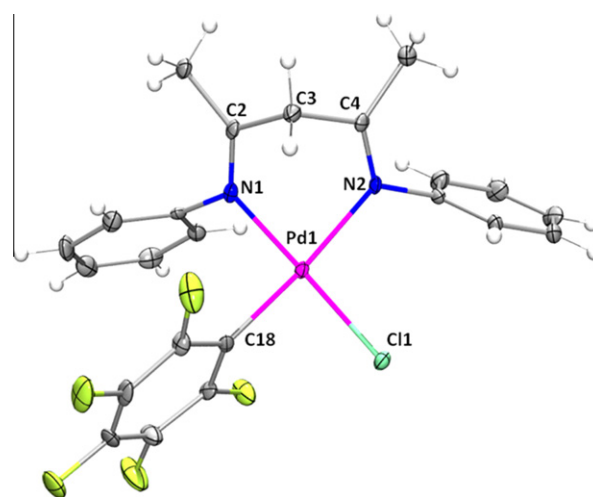
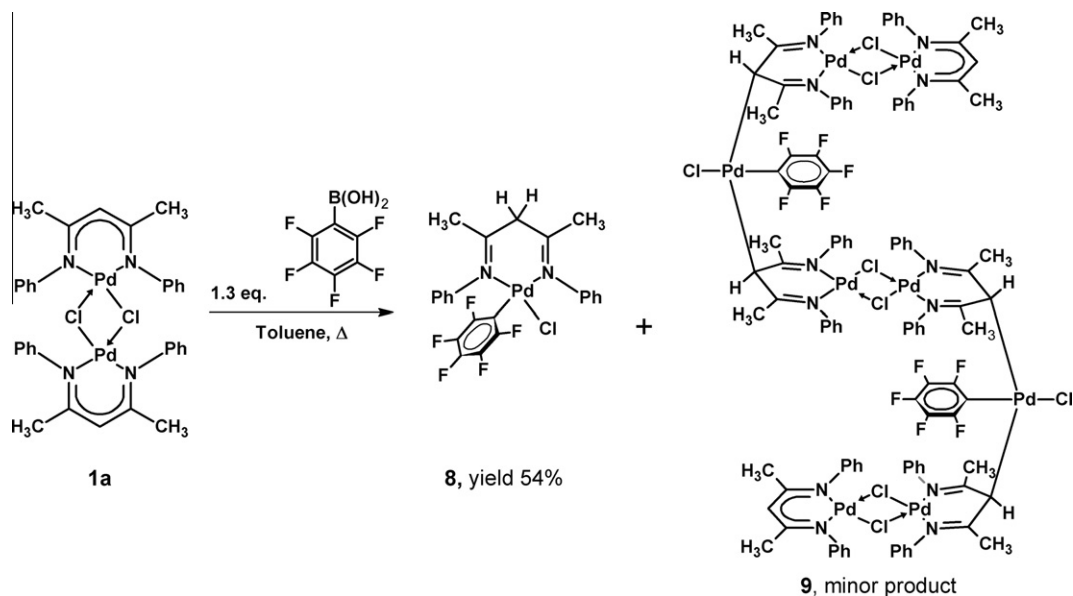


**Fig. 10.** Molecular structure of **8** with 30% probability ellipsoids. Hydrogen atoms are shown as spheres of arbitrary radius. Selected bond lengths (Å) and angles (°) for **8**: Pd1–N1, 2.029(3); Pd1–N2, 2.119(3); Pd1–C18, 2.002(4); Pd1–Cl1, 2.2896(10); N1–Pd1–N2, 86.74(13); C18–Pd1–Cl1, 89.91(12); N2–Pd1–Cl1, 94.32(9); C18–Pd1–N1, 89.15(15).

chloride they are *trans* to each other, and two  $\beta$ -C-donors from [Ph<sub>2</sub>nacnac]<sup>−</sup> are *trans* to each other. The Pd3–C20 and Pd3–C43 bond lengths are 2.179(6) and 2.167(5) Å, respectively, which are longer than other Pd–( $\beta$ -C) bond lengths such as in **7a**, **7b** and other



**Scheme 10.** Synthesis of **8**, and trace amounts of **9**.

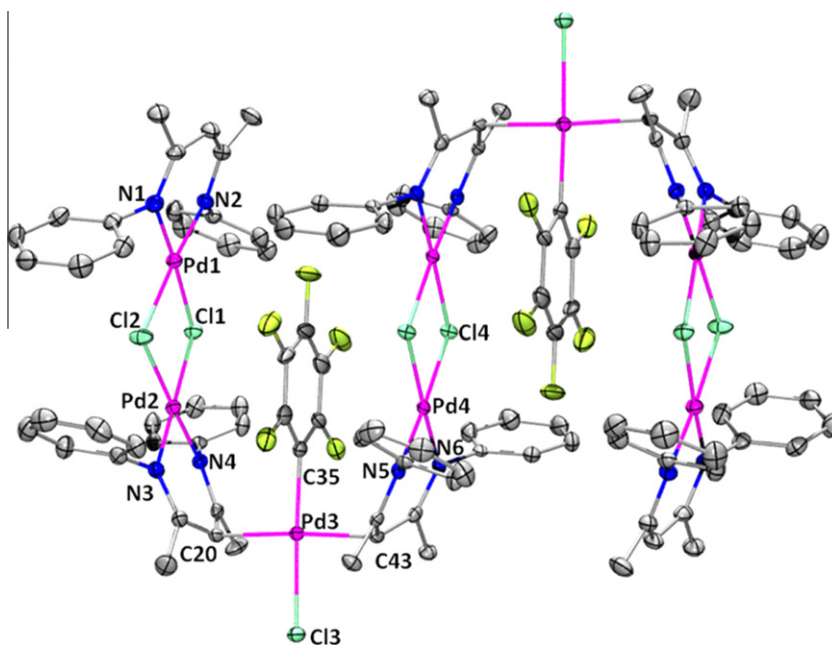


**Fig. 11.** Molecular structure of **9** with 30% probability ellipsoids. Hydrogen atoms are omitted for clarity. Selected bond lengths (Å) and angles (°) for **9**: Pd1–N1, 2.000(5); Pd1–N2, 1.984(5); Pd1–Cl1, 2.3508(15); Pd1–Cl2, 2.3321(16); Pd2–N3, 2.019(5); Pd2–N4, 2.008(5); Pd2–Cl1, 2.3263(14); Pd2–Cl2, 2.3175(16); Pd3–C35, 1.995(6); Pd3–C43, 2.167(5); Pd3–C20, 2.179(6); Pd3–Cl3, 2.3870(15); Pd4–N5, 2.000(5); Pd4–N6, 2.007(5); Pd4–Cl4, 2.3409(14); N2–Pd1–N1, 91.0(2); Cl2–Pd1–Cl1, 81.63(5); N1–Pd1–Cl2, 93.05(15); N2–Pd1–Cl1, 94.27(15); Pd2–Cl1–Pd1, 96.94(5); Pd2–Cl2–Pd1, 97.70(6); N4–Pd2–N3, 91.8(2); Cl2–Pd2–Cl1, 82.47(5); N3–Pd2–Cl2, 92.73(15); N4–Pd2–Cl1, 93.07(14); C35–Pd3–C43, 89.7(2); C35–Pd3–C20, 93.4(2); C43–Pd3–Cl3, 88.69(15); C20–Pd3–Cl3, 88.23(16); N5–Pd4–N6, 89.39(18); N5–Pd4–Cl4, 94.49(14); N6–Pd4–Cl4, 93.81(13).

examples mentioned previously [4,7,8]. Compound **9** is intriguing, not only due to its intrinsic beauty but also because it possesses Pd(II) centres with three carbon donors which is a rare feature, there are some examples such as complexes with bis-carbenes [35], or CCC-pincers [36], or bis-isocyanide ligands [37].

#### 4. Conclusions

In conclusion we have demonstrated the syntheses and characterization of several  $[\text{Pd}(\text{Ar}_2\text{nacnac})(\mu\text{-Cl})_2]$  complexes (**1a–1c**).

These chloro-bridged dimers can be used to generate mononuclear complexes when the chloride bridge is cleaved by monodentate ligands such as pyridine to form complexes **4a–4c**. Phenylboronic acid can also act as pyridine abstraction reagent from complex **4a** to form complex **1a**. Also these chloro-bridged dimers engage in unusual transmetalation reactivity with arylboronic acids to form tetrapallada-macrocycles **7a** and **7b**. Divergent transmetalation reactivity was encountered when **1a** was reacted with pentafluorophenylboronic acid, complex **8** and a trace amount of complex **9** formed selectively. We also demonstrated the

non-innocent and reactive nature of  $\beta$ -C in palladium ncnac complexes, where this backbone carbon can act both a carbon-donor as in tetrapallada-macrocycles **7a**, **7b** and also in complex **9**, or activate dioxygen to form complex **5**.

### Acknowledgements

We thank the Natural Science and Engineering Research Council of Canada (NSERC), the Canadian Foundation for Innovation (CFI), the Ontario Ministry of Research and Innovation and the University of Toronto for funding. V.T.A. gratefully thanks the NSERC for a postgraduate scholarship. R.T. gratefully thanks the Government of Ontario for an Ontario Graduate Scholarship.

### Appendix A. Supplementary material

CCDC 849170–849181 contain the supplementary crystallographic data for this paper. These data can be obtained free of charge from The Cambridge Crystallographic Data Centre via [www.ccdc.cam.ac.uk/data\\_request/cif](http://www.ccdc.cam.ac.uk/data_request/cif). Supplementary data associated with this article can be found, in the online version, at [doi:10.1016/j.ica.2011.09.044](https://doi.org/10.1016/j.ica.2011.09.044).

### References

- [1] For reviews on  $\beta$ -diiminato chemistry see: (a) L. Bourget-Merle, M.F. Lappert, *J. Severn, Chem. Rev.* 102 (2002) 3031; (b) D.J. Mindiola, *Angew. Chem., Int. Ed.* 48 (2009) 6198; (c) P.L. Holland, *Acc. Chem. Res.* 41 (2008) 905; (d) H.W. Roesky, S. Singh, V. Jancik, V. Chandrasekhar, *Acc. Chem. Res.* 37 (2004) 969; (e) W.E. Piers, D.J.H. Emslie, *Coord. Chem. Rev.* 131 (2002) 233.
- [2] X. Tian, R. Goddard, K. Pörschke, *Organometallics* 25 (2006) 5854.
- [3] M. Kang, A. Sen, *Organometallics* 24 (2005) 3508.
- [4] J. Feldman, S.J. McLain, A. Parthasarathy, W.J. Marshall, J.C. Calabrese, S.D. Arthur, *Organometallics* 16 (1997) 1514.
- [5] B. Lin, K.X. Bhattacharyya, J.A. Labinger, J.E. Bercaw, *Organometallics* 28 (2009) 4400.
- [6] A. Hadzovic, D. Song, *Organometallics* 27 (2008) 1290.
- [7] A. Hadzovic, J. Janetzko, D. Song, *Dalton Trans.* (2008) 3279.
- [8] V.T. Annibale, L.M. Lund, D. Song, *Chem. Commun.* 46 (2010) 8261.
- [9] L. Tang, Y. Duan, X. Li, Y. Li, *J. Organomet. Chem.* 691 (2006) 2023.
- [10] M. Stender, R.J. Wright, B.E. Eichler, J. Prust, M.M. Olmstead, H.W. Roesky, P.P. Power, *J. Chem. Soc., Dalton Trans.* (2001) 3465.
- [11] D.S. Laitar, C.J.N. Mathison, W.M. Davis, J.P. Sadighi, *Inorg. Chem.* 42 (2003) 7354.
- [12] G.K. Anderson, M. Lin, A. Sen, E. Gretz, *Inorg. Synth.* 28 (1990) 60.
- [13] R. Usón, J. Forniés, F. Martínez, M. Tomás, *J. Chem. Soc., Dalton Trans.* (1980) 888.
- [14] H.J. Frohn, N.Y. Adonin, V.V. Bardina, V.F. Starichenko, *Z. Anorg. Allg. Chem.* 628 (2002) 2827.
- [15] B.V. Nonius, *Collect. Data collection software* 1997.
- [16] Z. Otwinowski, W. Minor, *Methods Enzymol* 276 (1997) 307.
- [17] Apex 2 Software Package; Bruker AXS, Inc. 2008.
- [18] G.M. Sheldrick, *Acta Crystallogr., Sect. A: Found. Crystallogr.* 64 (2008) 112.
- [19] F. Barrios-Landeros, B.P. Carrow, J.F. Hartwig, *J. Am. Chem. Soc.* 131 (2009) 8141.
- [20] A. Hadzovic, D. Song, *Inorg. Chem.* 47 (2008) 12010.
- [21] R. Usón, J. Forniés, P. Gimeno, P. Espinet, R. Navarro, *J. Organomet. Chem.* 81 (1974) 115.
- [22] P. Espinet, J.M. Martínez-Illarduya, C. Pérez-Briso, A.L. Casado, M.A. Alonso, *J. Organomet. Chem.* 551 (1998) 9.
- [23] T. Koizumi, A. Yamazaki, T. Yamamoto, *Dalton Trans.* (2008) 3949.
- [24] S. Yokota, Y. Tachi, S. Itoh, *Inorg. Chem.* 41 (2002) 1342.
- [25] J.D. Azoulay, R.S. Rojas, A.V. Serrano, H. Ohtaki, G.B. Galland, G. Wu, G.C. Bazan, *Angew. Chem., Int. Ed.* 48 (2009) 1089.
- [26] M.L. Scheuermann, U. Fekl, W. Kaminsky, K.I. Goldberg, *Organometallics* 29 (2010) 4749.
- [27] R.H. Crabtree, *The Organometallic Chemistry of the Transition Metals*, John Wiley and Sons, Inc., Hoboken, New Jersey, 2005.
- [28] T. Sciarone, C. Nijhuis, A. Meetsma, B. Hessen, *Dalton Trans.* (2006) 4896.
- [29] M. Walter, R. Moorhouse, S. Urbin, P. White, M. Brookhart, *J. Am. Chem. Soc.* 131 (2009) 9055.
- [30] H.R. Snyder, M.S. Konecky, W.J. Lennarz, *J. Am. Chem. Soc.* 80 (1958) 3611.
- [31] D.L. Yabroff, G.E.K. Branch, *J. Am. Chem. Soc.* 55 (1933) 1663.
- [32] D.G. Hall, *Boric Acide Preparation, Applications in Organic Synthesis and Medicine*, WILEY-VCH Verlag GmbH & Co. KGaA, Weinheim, 2005.
- [33] F. Blank, H. Scherer, J. Ruiz, V. Rodríguez, C. Janiak, *Dalton Trans.* 39 (2010) 3609.
- [34] R.P. Hughes, A.J. Ward, J.A. Golen, C.D. Incarvito, A.L. Rheingold, L.N. Zakharov, *Dalton Trans.* (2004) 2720.
- [35] E.A. Couzijn, E. Zocher, A. Bach, P. Chen, *Chem. Eur. J* 16 (2010) 5408.
- [36] Z. Liu, T. Zhang, M. Shi, *Organometallics* 27 (2008) 2668.
- [37] L.A. Labios, M.D. Millard, A.L. Rheingold, J.S. Figueroa, *J. Am. Chem. Soc.* 131 (2009) 11318.